T.C.
ISTANBUL AYDIN UNIVERSITY
INSTITUTE OF GRADUATE STUDIES

PASSIVE ISLANDING DETECTION TECHNIQUE FOR THREE-PHASE GRID-CONNECTED PV INVERTER SYSTEM

MASTER'S THESIS

Mohammad-Yassine EL HASSNI

Department of Electrical and Electronic Engineering
Electrical and Electronics Engineering Program

JULY, 2021

T.C.
ISTANBUL AYDIN UNIVERSITY
INSTITUTE OF GRADUATE STUDIES

PASSIVE ISLANDING DETECTION TECHNIQUE FOR THREE-PHASE GRID-CONNECTED PV INVERTER SYSTEM

MASTER'S THESIS

Mohammad-Yassine EL HASSNI
(Y1813.300011)

Department of Electrical and Electronic Engineering
Electrical and Electronics Engineering Program

Thesis Advisor: Prof. Dr. Murtaza FARSADI

JULY, 2021

APPROVAL PAGE

DECLARATION

I hereby declare with respect that the study “Passive Islanding Detection Technique for Three-phase grid-connected PV inverter system”, which I submitted as a Master thesis, is written without any assistance in violation of scientific ethics and traditions in all the processes from the Project phase to the conclusion of the thesis and that the works I have benefited are from those shown in the Bibliography. (01/07/2021)

Mohammed-Yassine EL HASSNI

FOREWORD

I would like to start by thanking God, my father Hamid El Hassni, my Mother Rkia Ramid, my brother Oussama El Hassni, Patrycja Kubala as well as my friends who have been supportive and patient and encouraging throughout all the ups and downs making sure that I remain the good man, as well as the positive member of society they envisioned me to be. And I pray to God that I always make them proud and happy while never letting them down in any manner. I would like to thank my thesis advisor Prof. Dr. Murtaza Frasadi of Electric and Electronic Engineering department at Istanbul Aydin University. The door to Prof. Murtaza Frasadi's office was always open whenever I ran into a trouble spot or had a question. He consistently allowed this paper to be my own work but steered me in the right direction whenever he thought I needed it. I would also like to thank my co-advisor during the exchange year in Poznan University of Technology Dr. Eng. Arkadiusz Dobrzycki for allowing me to do my research under his supervision and pointing me to the right direction through my research. I would like to thank all my teachers for having great influence on me, I would also like to thank department of Electric and Electronic Engineering as well as Istanbul Aydin University and its library for providing me with access to all the books and articles that I needed to finish this work.

July, 2021 Mohammed-Yassine EL HASSNI

PASSIVE ISLANDING DETECTION TECHNIQUE FOR THREE-PHASE GRID-CONNECTED PV INVERTER SYSTEM

ABSTRACT

In this paper, we explore a passive Islanding detection Method (IDM) that relies on the passive feedback built in One Cycle Control (OCC) inverter driving the Voltage at the Point of Common Coupling (VPCC) outside normal range of operation during an islanding condition without relying on additional computational effort or injection of external disturbance into the grid. The method tested on a three-phase grid-Connected inverter that is incorporated. The Pseudo-state-charge concept is explained in order to attain a better energy management and storage. In addition, the paper explores a PV plant control strategy that is not invasive to the inverter and based on the remote control of the PV-Strings actuators that is eventually applied on a microgrid-based smart grid.

Keywords: photovoltaic systems, one cycle control, islanding detection, feedback, passive islanding detection method. Distributed generation, energy storage management, renewable energy sources, smart grid, smart microgrid.

ÜÇ FAZLI ŞEBEKE BAĞLANTILI PV EVIRICI SISTEMI IÇIN PASIF ADALANMA ALGILAMA TEKNIĞI

ÖZET

Bu tezde, bir ada oluşturma durumu sırasında Ortak Kuplaj Noktasındaki (VPCC) Gerilimi normal çalışma aralığının dışında çalıştıran Tek Döngü Kontrollü (OCC) invertörde yerleşik pasif geri beslemeye dayanan pasif bir Adalama algılama Yöntemi (IDM) araştırıyoruz, ek hesaplama çabasına veya şebekeye harici rahatsızlık enjeksiyonuna dayanmadan. Yöntem, entegre edilmiş üç fazlı bir şebekeye bağlı evirici üzerinde test edilmiştir. Daha iyi bir enerji yönetimi ve depolaması elde etmek için sözde durum yükü kavramı açıklanmıştır. Ek olarak, makale, invertere müdahale etmeyen ve sonunda mikro şebeke tabanlı bir akıllı şebekeye uygulanan PV-Strings aktüatörlerinin uzaktan kontrolüne dayanan bir PV tesis kontrol stratejisini araştırıyor.

Anahtar Kelimeler: fotovoltaik sistemler, tek çevrim kontrolü, ada tespiti, geri besleme, pasif ada tespiti yöntemi. Dağıtılmış üretim, enerji depolama yönetimi, yenilenebilir enerji kaynakları, akıllı şebeke, akıllı mikro şebeke.

TABLE OF CONTENTS

ABBREVIATIONS

DG : Distributed Generation

IDM : Islanding Detection Method

MPPT : Maximum Power Point Tracking

OCC : One Cycle Control

OVP : Over Voltage Protectıon

PCC : Point of Common Coupling

PLL : Phase Locked Loop

PV : PhotoVoltaic

UVP : Under Voltage Protection

VPCC : Voltage at The Point of Common Coupling

LIST OF TABLES

LIST OF FIGURES

I. INTRODUCTION

It is no secret that during the last century we, as human beings, have affected our planet in a significantly bad way. Affecting every living creature on this planet, climate change has made us seek deferent routs to secure our daily energy needs.

During these last decades, the climate change and the jump of the oil prices have reinforced our sense of urgency to develop of the so-called renewable energy sources.

Photovoltaic (PV) and Wind energy production are popular nowadays, which made their demand-driven energy production required to be made without risking the power supply reliability and quality.

For the last few decades, average consumers have realized the cost effectiveness and the environment friendly nature of the grid connected photovoltaic (PV) distributed generation (DG) system that are usually single-phase system with a below 5kw power rating, causing a huge and significant increase in its number and demand.

The usage of one cycled control (OCC) in these DG systems proved to be simple, cost effective, responsive and phase locked loop (PLL)free grid synchronized.

A. Purpose

When a section of utility system that consists of a generation and load is isolated from the rest of the system yet remains energized, we have what we call an islanding condition. This condition that is often unintentional occurs during a grid failure. The islanding condition is considered as one of the most critical safety concerns in many studies carried out in order to find out the impact of the DGs on the safety and operation of the utility grid.

The purpose of this thesis is to detect the islanding mode without relying on additional computational effort or injection of external disturbance into the utility grid.

This is done by relying on a feedback-based passive Islanding Mode Detection, which is suitable for OCC based inverters.

By relying on the inbuilt feedback nature of the OCC scheme, the IDM principle is to drive the voltage at the point of common coupling (VPCC) outside the natural range of operation during the occurrence of the islanding condition.

In this thesis, we shall also look at what it seems to be one of the most important parts of future smart grids topologies that is the microgrid. The microgrid is usually established as a distribution grid that includes distributed generators, energy storage unites and loads that are controllable.

B. Solar Energy Concept and Benefits

Right from the start, the development of photovoltaic systems has had a lively and smooth characteristic, since the first discovery of the photovoltaic effect by Becquerel in 1839, to the first development of the first photovoltaic cell that had an efficiency lower than 1% by Fritz in 1883 and the newer photovoltaic cell that used a copper and semiconductor copper oxide which also had a below 1% efficiency, to the silicon photovoltaic cell developed by Ohl in 1941, which its refinement enabled researchers to attain a 6% efficiency in direct sunlight which was further increased to 11% by Bell Labs in 1954, to the increased demand of the improvement of photovoltaic power generation by the space program in 1960s.The scientist needed to find ways and solution to produce more power without worrying about the costs. Which changed later on upon depletion of natural resources of energy as I have mentioned earlier.

The development of the of photovoltaic systems has been managed both in R&D and demonstration fields.

The direct use of the heat absorbed from the radiation of the sun and directly convert sunlight to electricity with a simple solid state device, longevity with minimum maintenance needs and costs, effectiveness, reliability,

decentralized power production, versatility in power handling, high power weight ratio, adding the abundance, pollution free and renewability, the solar energy has become a promising alternative source of energy in the 21st century.

C. PV Power Generation System

Up until mid-90s, Most PV systems were standalone, and its applications were independent from the grid. the standalone off-grid frame works can be defined as producing power independently without relying on the utility grid, this type of framework can be seen in telecommunication units, remote stations, rural power supplies and auxiliary power units for military and medical station (as a back-up power supply). As for the grid connected systems, we can simply define them as the ones that are connected to the utility grid. These frameworks are mostly feeding the nearby load's necessity as their priority and flowing the surplus power into the grid. Some other grid connected frame works feed all the generated power to the utility grid without sparing any for the local loads. Since the UTILITY system gives limitless capacity control, the framework could manage huge load assortments.

Since 2005, the grid systems have persistently picked up market in view of government' progressions. Today they speak to about 75% of the overall PV market.

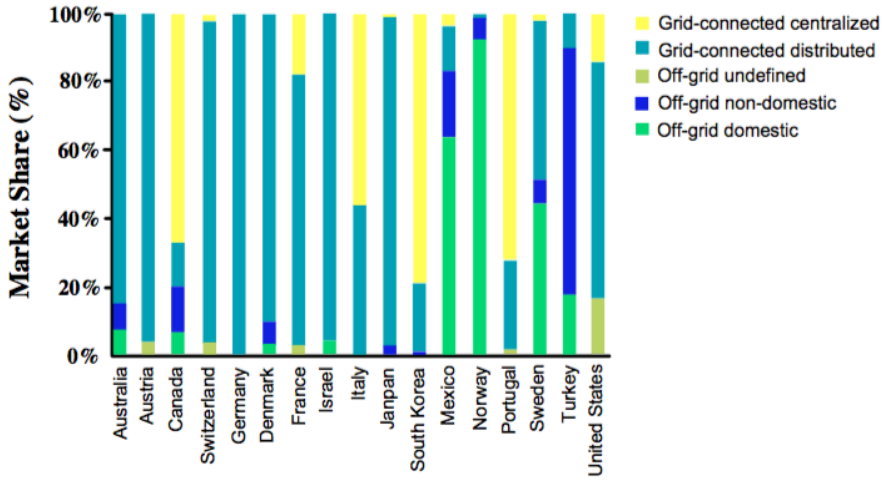

Figure 1. Market Share of Cumulative Installed PV Capacity, by Application

Source: IEA, 2011

D. Thesis Objectives

At the beginning of this research, the goal was to implement the Islanding Mode Detection method and run simulation looking to improve it. However, as I was developing the idea, I figured out it was best to implement the idea into a microgrid that is eventually connected to the utility grid as its back up. This is why I have touched on micro grid and energy storage management.

The thesis has the goal of widening the area of use of the OCC inverter, with a special innovative IDM. The goal was to move from a one phase inverter to a 3-phase inverter and eventually implement a load and energy management technique that could allow us to take as much advantage of the harnessed energy from the sun and the winds.

The wind energy was not touch upon as it was not the main focus of this thesis.

II. PHOTOVOLTAIC SYSTEMS

A. Brief History of the Photovoltaic System

In 1839, the French physicist Alexander Edmond Becquerel (1820-1891) discovered the photovoltaic effect while working while experimenting with a solid electrode in an electrolyte solution[1]. In his experiment, 19-year-old Edmond Becquerel placed a silver chloride in an acidic solution, connected the platinum electrodes and shined light on them. During this experiment Becquerel noticed that a voltage has developed when the electrodes were illuminated. In 1848, English electrical engineer Willoughby Smith discovered the photo conductivity in selenium which by lead to the invention of photoelectric cells. During his experiments, Smith discovered that selenium rods conductivity significantly increased when exposed to sunlight that his described it as “Effect of Light on Selenium During the Passage of An Electric Current" in an article published in the February 1873 issue of Nature. During the 1870s, Professor Williams Grylls Adams and his student Richard Evans Day of Kings College proved that it is possible to convert solar energy directly into electricity with no need for any moving parts nor heat by subjugating selenium to several experiments. One of those trials was the candle experiments, where they lit a candle an inch away from the same bar of selenium Willoughby had used. The needle on their measuring device would rise instantly when the selenium was exposed to the candlelight and drop to zero immediately to zero one selenium is screened from it. This ruled out the thermal electricity possibility. They eventually concluded “it was clear that a current could be started in the selenium by the action of the light alone.”. Adams and Days called this newly discovered current that is produced by light ‘‘photoelectric’’ but modern-day scientist refer to the phenomenon as the “photovoltaic effect”.

In 1883, American inventor Charles Edgar Fritts invented the first real working solar module. This module was made by coating a wide copper plate with selenium and then an extremely thin semi-transparent layer of gold leaf

was placed on top. According to Fritts reports, the module produced a current “that is continuous, constant, and of considerable force”. Beside the sunlight, the current reportedly responded to dim daylight and even candlelight that made him suggest "we may see the photoelectric plate competing with (coal fired) fossil fuel plants"[2].

It took about 70 years to make another breakthrough in the development of the photovoltaic technology. This long drought like period was caused by what Albert Einstein believed was a failure to understand all the energy streaming from the sun on the scientists’ behalf. Einstein’s novel description of light in his infamous paper in 1905 about the packets of energy the light contains also known as quanta (now called photons) combined with the discovery of the electron and the rash of research into its behavior provided photoelectricity with a scientific framework it had previously lacked. It was finally possible to explain the phenomenon with words that science can understand. The phenomenon was defined as follows: In semiconductor materials, photons can knock electrons from their atomic orbits and, if connected properly by a circuit, could generate enough electricity to do "work". In 1913 William Coblentz received the first US Patent (1077219) to convert sunlight into electricity.

The drought was essentially ended by a slightly modified wafer of silicon that was named solar cell. This solar cell converted sunlight directly into electrical energy at an efficiency of just 6% was unveiled in 1954 by Bell telephone Laboratories in Murray Hill, NJ. The inventors were: Gerald L. Pearson, Daryl M. Chapin, and Calvin S. Fuller. The New York Times subsequently forecasted that solar cells would eventually lead to a source of "limitless energy of the sun.". The solar cell operates on the same principle that underlies the transistor where a junction is set up in silicon crystal (explained in detail in following sections).

At first, the solar power was not used as mainstream energy source due to its high price (300$/watt solar module). However, the space war between the USA and the Soviet Union in the 60s and the 70s benefited from the solar cell as they were used to power earth orbiting satellites such as the VANGUARD I and the EXPLOERE-6.

Thanks to the much cheaper solar module design from Dr. Elliot Berman in the 1970s, solar power was brought down from outer space satellites to earth bound applications. The design used a less pure grade of silicon (rejects from semiconductors) and manufacturing techniques from similar to that of photographic film. This brought down the price to $20 per watt. Figure 4.1 below shows the earlier development of the photovoltaic on a simplified timeline.

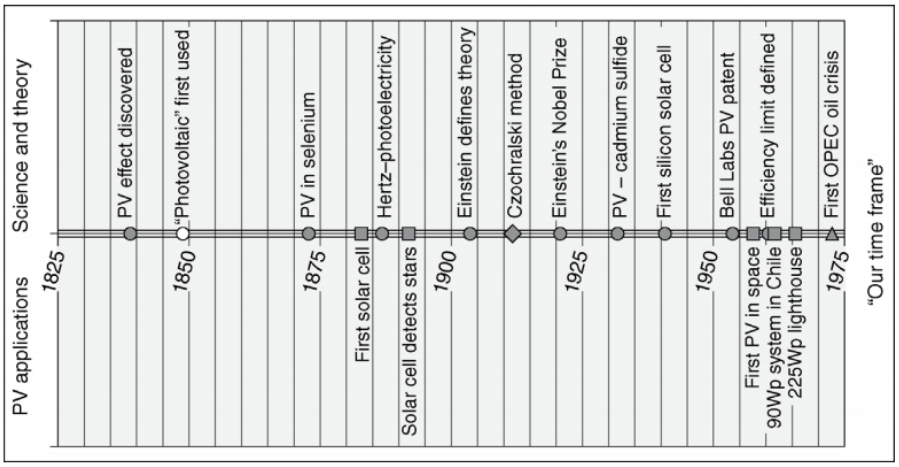

Figure 2. Simplified Timeline of Earlier Photovoltaics Development.

With the cost of solar cells well within everyone's budget, solar power has never looked so tempting as we see solar cells in a wide variety of places today. These places may be a household, cars and there is even a solar powered aircraft that has flown higher than almost any other aircraft.

B. How do Solar Cells Work?

The energy from the Sun is the most abundant and absolutely freely available energy on planet earth. In order to utilize this energy, we need help from the second most abundant element on earth, sand. The sand must be converted to 99.999% pure silicon crystals to use in solar cells. o achieves this, the sand has to go through a complex purification process that is basically cooking sand with carbon at a 2000° C in order to get raw silicon at 98% purity rate. The raw silicon gets converted into a gaseous silicon compound form that is then mixed with hydrogen to get highly purified polycrystalline silicon SiHcl3. These silicon ingots are reshaped and converted into very thin slices called silicon wafers. The silicon wafer is the heart of a photovoltaic cell. When

we analyze the structure of the silicon atoms you can see they are bonded together where the electrons in this structure have no freedom of movement.

Let's consider a 2d structure of the silicon crystals. Assume that phosphorus atoms with five valence electrons are injected into it. This results in one electron that, in this structure, will free provided it get sufficient energy. Let's try to make a highly simplified solar cell only using this type of material. When light strikes them, the electrons will gain photon energy and will be free to move. However, this movement of the electrons is random. It does not result in any current through the load. To make the electron flow unidirectional a driving force is needed.

An easy and practical way to produce the driving force is a PN junction. Similar to n-type doping if you inject boron with three valence electrons into pure silicon there will be one hole for each atom which we call p-type doping. If these two kinds of doped materials join, some electrons from the N side will migrate to the P region and fill the holes available there. This way a depletion region is formed where there are no free electrons and holes (figure 3). Due to the electron migration the N-side boundary becomes slightly positively charged. And the P side becomes negatively charged. An electric field will be formed between these charges. This electric field produces the necessary driving force.

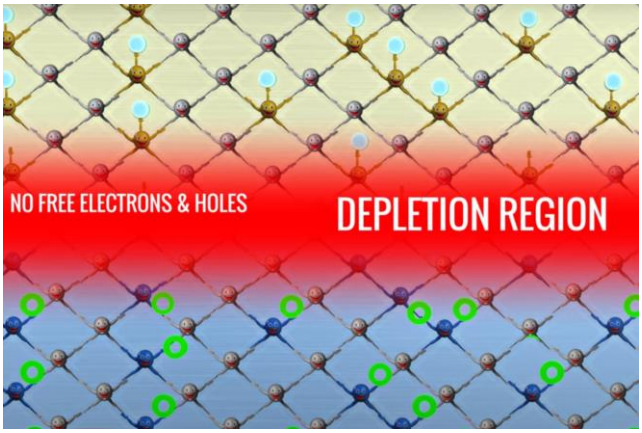

Figure 3. PN Junction Diagram

To explain it in a more detailed manner, When the light strikes the PN Junction something very interesting happens. Light strikes the N region of the PV cell and it penetrates and reaches up to the depletion region where the electric field drives them out of it. Eventually, the concentration of electrons in

the N region and holes in the P region become so high that a potential difference will develop between them. As soon as we connect any load between these regions, electrons will start flowing through the load and will recombine with the holes in the P region after completing their path. In this way a solar cell continuously gives direct current.

In a practical solar cell, the top N layer is very thin and heavily doped while the P layer is thick and lightly doped in order to increase the performance of the cell. In a practical solar cell, the thickness of the depletion region is usually high. Which means that when illuminated, the electron hole pairs are generated in a wider area, and by consequence more current generation by the PV cell. The other advantage is that due to the thin top layer, more light energy can reach the depletion region.

C. How does a PV System Work?

If we were to look at the PV frameworks in a general fashion, we will see that it resembles other electrical power generating methods, just the hardware utilized is quite different from that of a regular electromechanical energy producing frameworks. With that being said, the standard of activity and interfacing with other electrical frameworks continue the same way as it always had with the same settled assortments and of electrical codes and standards in place.

The PV array/Module produce power when exposed to the sunlight. However, in order control, convert, convey, and store the energy harnessed from the sun by the array, various components are required.

As every system has its functional and operational requirements, the specific components for required in a PV system may include significant segments such as DAC-AC inverter, battery bank, system and battery control, additional assistant energy source and even specific electrical loads (appliance) sometimes. What's more, a collection of Balance of System (BoS) equipment, including wiring, overcurrent, flood security and detach gadgets, and other power processing hardware. Figure 4. shows a fundamental graph of a photovoltaic framework.

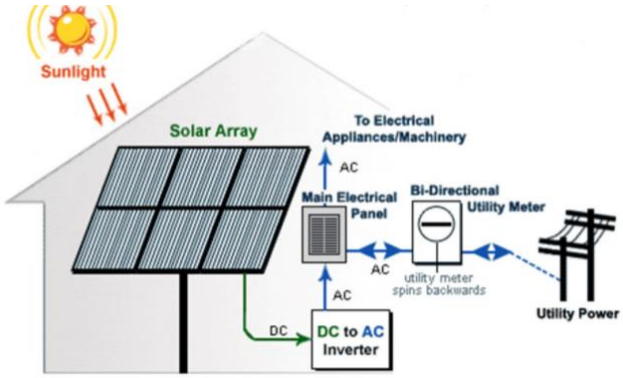

Figure 4. Major PV System/Framework

D. Modeling of PV Module/Array in MATLAB/ Simulink

Considered as the building block of PV array, the solar cell is basically a p-n semiconductor junction that converts light energy directly into electricity. Figure 4 shows the ideal, practical, and simplified models if single diode model of PV cell. Having a minimal output power in the order of 200W and a corresponding voltage between 25 and 40V, the PV module is typically composed of 30-50 cells in series connection. The interconnection of these PV modules in series and parallel or any other connection form gives us what is defined as PV array. The PV system energy production is totally dependent on the solar irradiance and temperature.

The mathematical representation of defining the I-V characteristics of PV array with ns cells connected in series is given in the equation below [3]:

$$I_{PV}=I_{PH}N_P - I_rN_P\,[\,\exp((V_{PV} + R_S()I_{PV})/\,V_Ta) -1\,] - (V_{PV} + R_S()I_{PV})/\,R_{sh}\,())$$

Equation 1

Where:

- I_{PH} is photo current generated due to incident solar irradiance [A]
- I_r is diode reverse leakage current [A]
- I_{PV} is terminal current [A]
- V_{PV} is terminal voltage
- V_T is thermal voltage; VT = (ns x k x T)
- k is Boltzmann's constant; k= 1.3806503x10−23 J/K
- T is the operating temperature in Kelvin [k]
- q is the charge of an electron; q = 1.60217646 x10−19 C

- R_s is the series resistance
- R_{sh} is the shunt resistance
- N_S is the number of modules connected in series in an array
- N_P is the number of modules connected in parallel in an array
- n_s is the number of cells in series in PV module
- a is the diode emission coefficient or ideality factor (ideal value is a=1)

For the modeling of a PV array N_s and N_P were selected as 1. I_{PH} the photo generated current in the PV module is dependent on the solar irradiance while being influenced by the operating temperature as shown in the equation 2.

$$I_{PH} = (G/G_{STC})(I_{PH,STC} + k_I \Delta_T)\ldots$$

Equation 2

Where G_{STC} is the irradiance at standard test condition (STC) measured in [W/m2], G is the irradiance on the PV module surface, K_I is the temperature coefficient of the short-circuit current (A/K), IPH,STC is the generated photo current at standard test condition, and Δ_T= T-T_{STC} where T and T_{STC} are the actual and STC temperature measured in Kelvin [K]. The diode reverse leakage current, Ir strongly depends on the temperature and is given in the equation below;

$$I_r = \frac{I_{SC,STC} + K_I \Delta_T}{\exp((V_{OC,STC} + K_V \Delta_T)/\alpha V_T) - 1}$$

Equation 3

Where $I_{SC,\,STC}$ [A] is the short-circuit current at STC; $V_{OC,\,STC}$ is the open-circuit voltage at STC; K_V is the temperature coefficient of open-circuit voltage [V/K].

Using the three equations mentioned above, an equivalent circuit, simulation model, and detailed modeling of OV module in MATLAB/Simulink environment to obtain the I-V and P-V characteristics were acquired and shown in Figure 5, b, c, d. A single diode model of PV cell is considered in order to obtain better accuracy and ease of mathematical calculations to estimate the series and shunt resistances of the PV model.

Based in the 1st equation above, we shall demonstrate how the series and shunt resistances are calculated in order to describe the relationship between the PV module operating voltage and current as follow.

- The series and shunt resistances of PV module are estimated by using Eqs. (4)-(6). In Eq. (4); RS is also present in the logarithmic term, therefore an initial value of R_S, i.e. R_{S0} can be obtained by removing the logarithmic numerator terms of $I_{MP}.R_S$ and $a.V_T$ which is given by Eq. (6).

$$R_S = \frac{1}{I_{MP}}\left[V_{oc} - V_{MP} - a \cdot V_T \cdot \ln\left(\frac{V_{MP} + a \cdot V_T - I_{MP} \cdot R_S}{a \cdot V_T}\right)\right]$$

Equation 4

$$R_{S0} = \frac{1}{I_{MP}}\left[V_{OC} - V_{MP} - a \cdot V_T \cdot \ln\left(\frac{V_{MP}}{a \cdot V_T}\right)\right]$$

Equation 5

- The value of R_{S0} from Eq. (5) is inserted in Eq. (4) to obtain the value of R_{S1}. If it is wished to improve the result, this process is repeated for several times, i.e. the value of R_{S1} is again inserted in Eq. (4) to obtain R_{S2}. In most cases, in the third or fourth iteration process, the values of R_{S3} and R_{S4} are relevant and can be taken as final values of R_{Sf}.
- As soon as the value of R_{Sf} is determined, the value of shunt resistance can be estimated by using Eq. (6).

$$R_{SHf} = \frac{(V_{MP} - a \cdot V_T) \cdot (V_{MP} - I_{MP} \cdot R_S)}{(I_{SC} - I_{MP}) \cdot (V_{MP} - I_{MP} \cdot R_S) - (I_{MP} \cdot a \cdot V_T)}$$

Equation 6

- The maximum values of R_{Sf} and minimum values of R_{SHf} under various irradiance levels are determined by Eq. (7) and (8).

$$R_{Sf,\max} = \frac{V_{OC,STC} - V_{MP}}{I_{MP}}$$

Equation 7

$$R_{SHf,\min} = \frac{V_{MP}}{I_{SC,STC} - I_{MP}} - \frac{V_{OC,STC} - V_{MP}}{I_{MP}}$$

Equation 8

- The variations in final vales of R_{Sf} and maximum values of $R_{Sf,\,max}$; and the minimum values of $R_{SHf,\,min}$ and final values of R_{SHf} under various irradiance levels are shown in Figure 6 (a,b). The simulated I-V and P-V characteristics of KC200GT PV module operating at constant temperature of 25°C and various irradiance levels are shown in Figure 7 (a,b).

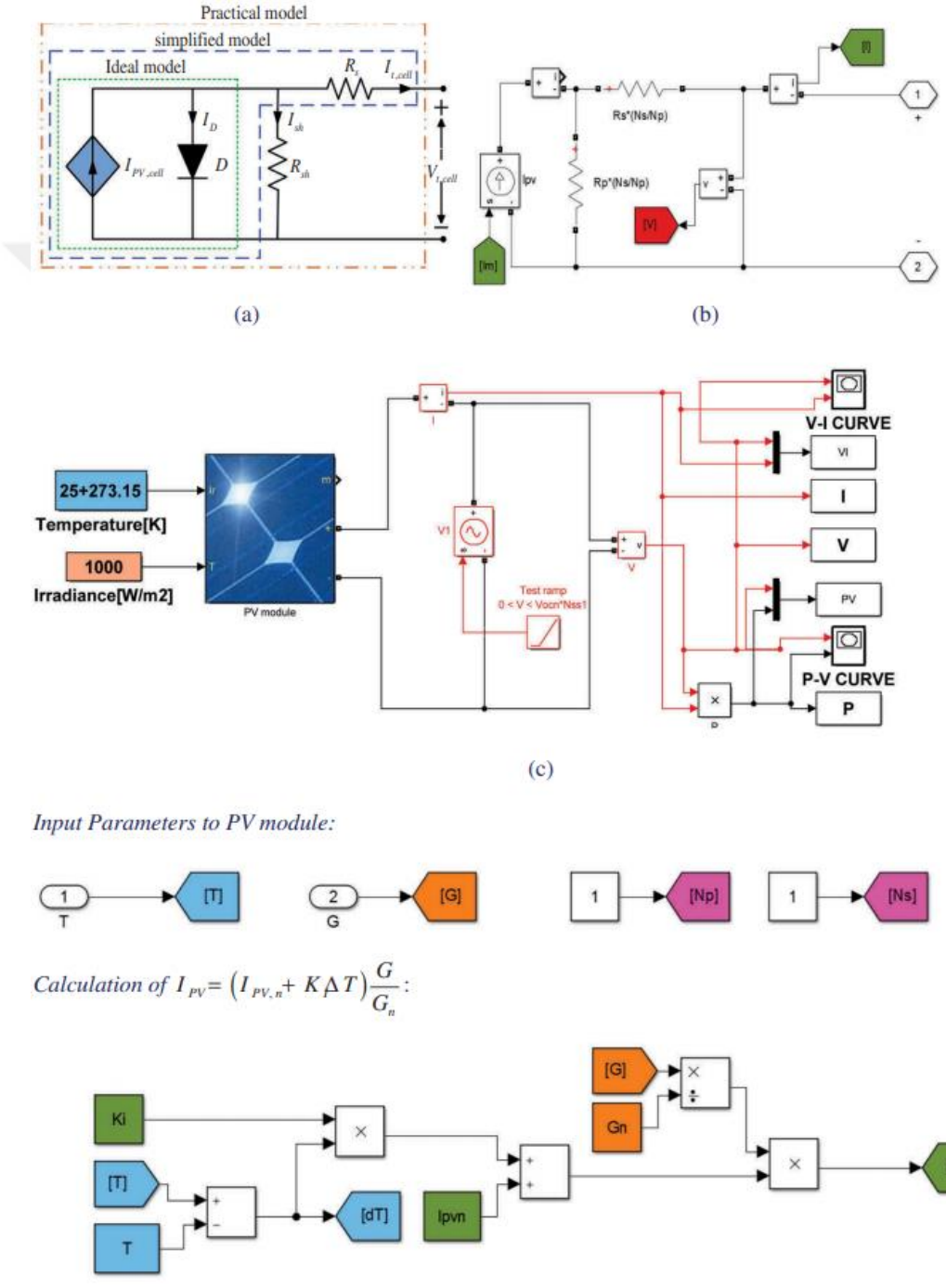

Figure 5. Modeling of PV Module in MATLAB/Simulink (a) Different Models of PV Cell, (b) Equivalent Circuit of PV Module (c) Simulating the Output Power,

Voltage, Current, and I-V and P-V Characteristics of PV Module (d) Detailed Mathematical Modeling of PV Module.

$$Calculation\ of\ I_r = \frac{I_{sc,n} + K_I \Delta_T}{\exp\left(\frac{V_{oc,n} + K_V \Delta_T}{aV_T}\right) - 1}:$$

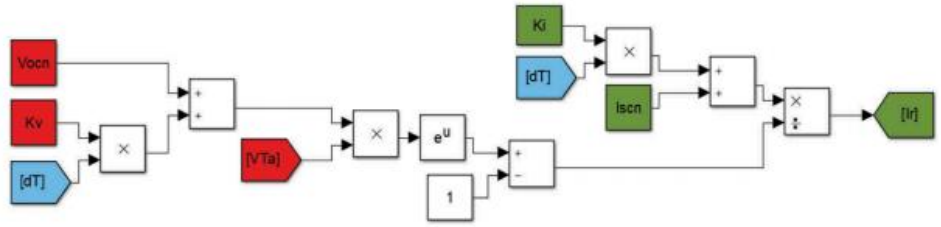

$$\text{Calculation of } I_m = I_{PH} - I_d = \left(I_{PV,n} + K_I \Delta_T\right)\frac{G}{G_n} - I_r\left[\exp\left(\frac{q(V + R_S I)}{n_s kTa}\right) - 1\right] - \frac{V + R_S I}{R_{SH}}:$$

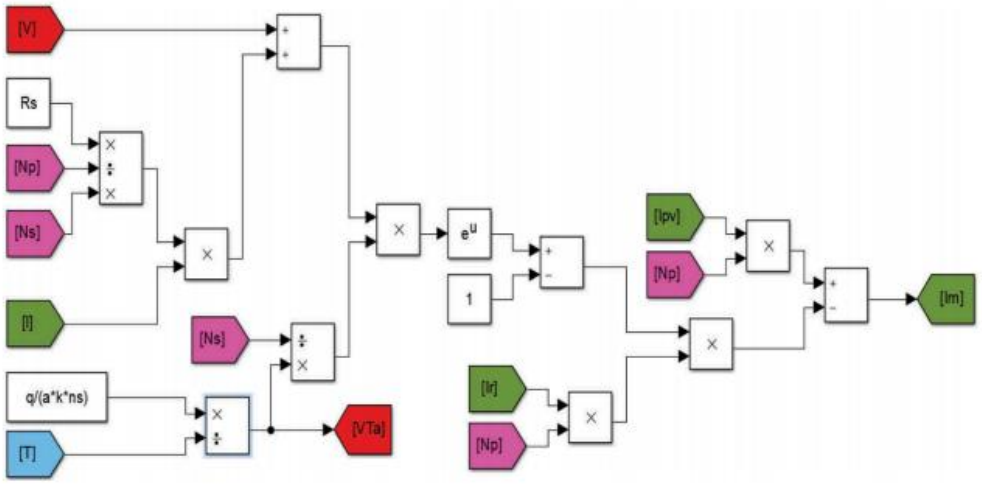

(d)

Figure 5 (continued)

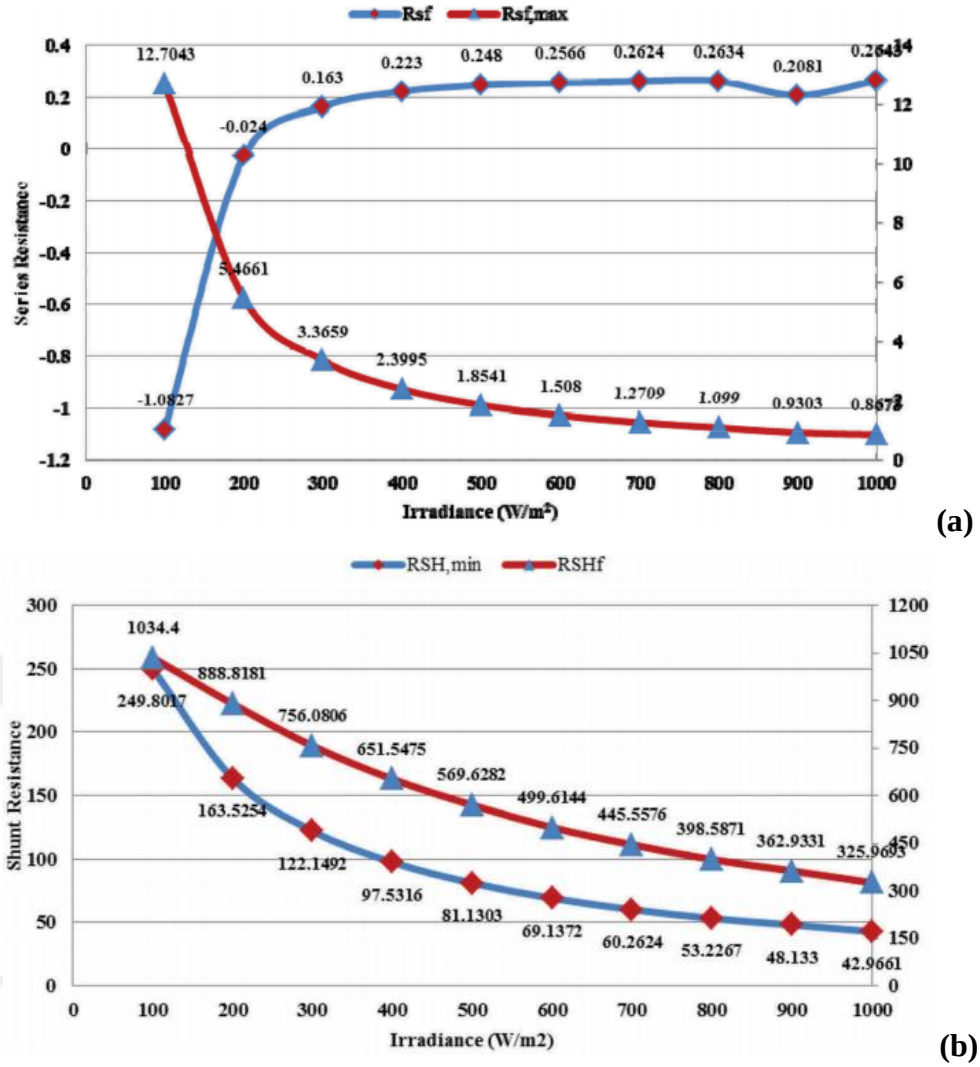

Figure 6. Series and Shunt Resistances of PV Module Under Various Irradiance Levels, (a) Variations in Final and Maximum Value of R_S, (b) Variations in Minimum and Maximum Value of R_{SH}.

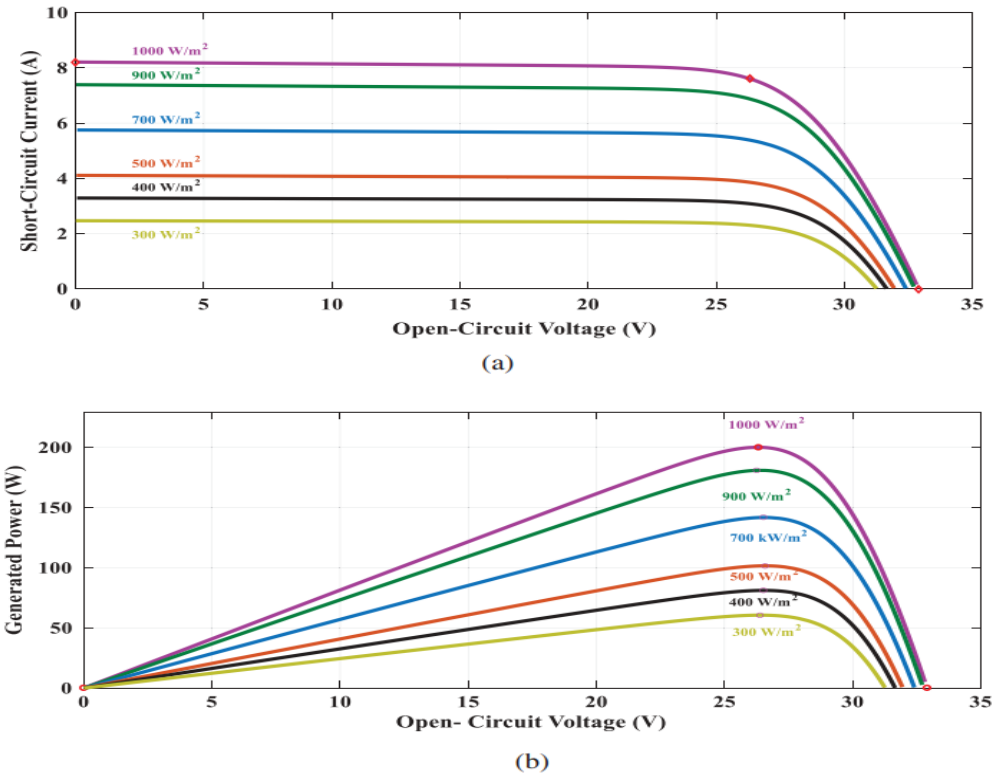

Figure 7. Output Characteristics of KC200GT PV Module at Different Irradiance Levels. (a) I-V Characteristics and (b) P-V Characteristics.

E. Control Algorithm for MPPT Perturbation and Observation Technique

Maximum Power Point Tracking (MPPT) is an algorithm that is implemented in PV inverters in order to adjust the impedance seen by the solar array in continuous fashion to keep the PV system operating at, or close to, the peak power point of the PV panel under changing conditions such as solar irradiance, temperature and load.

As it is already known the temperature and irradiance of the sun is forever changing throughout the day. Which means that at every time times the temperature and irradiance condition change, the Current Voltage curve (I-V curve) that is defined for this condition changes as well. Consequently, the power voltage curve (P-V curve) changes as well. The operating power on the P-V curve will correspond to an operating point on I-V curve. The P in the P-V curve stands for the power delivered to the rest of the PV system and eventually the load. Therefore, it is advantageous to operate the solar modules at maximum power that is the peak point of the P-V curve. See figure 8 below.

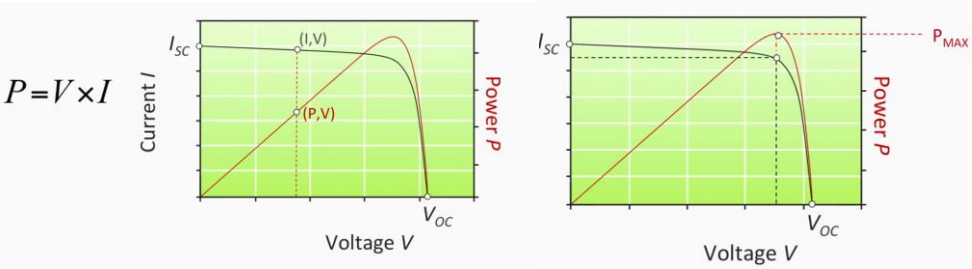

Figure 8. I-V and P-V Curves Showing Operating Point and Maximum Power Point

With no external electrical interference and manipulation, the PV module operating point is generally defined by the load at its output. However, in order to get maximum power delivered to the load at all time, it is imperative to force the module to operate at the operating point that corresponds to its maximum power that is also called the Maximum Power Point. The maximum power point corresponds to either the peak of the P-V curve or the knee of the I-V curve as seen in figure 8.

In order to have the PV module operating at the maximum power point, we simply have to force the its voltage to be the same as the voltage at the maximum power point or regulate the current to equal that of the maximum power point using converters.

As the ambient condition like irradiance or temperature are changing, and therefore causing the I-V and P-V curves to change as well, the old MPP is no longer valid. Thus, to continue to operate at maximum power point, we will need to track and detect any changes in the I-V curve and then find out the new MPP. This Process is called Maximum Power Point Tracking or MPPT.

The three most common MPPT algorithms are:

- Perturbation and observation (P&O)
- Incremental conductance
- Fractional open-circuit voltage

The P&O algorithm perturbs the operating voltage in order to guarantee maximum power. Although, this algorithm has several advanced and optimized variations [4], a basic P&O MPPT algorithm is shown in in figure 9.

On the other hand, the Incremental conductance algorithm, compares the incremental conductance (IΔ/VΔ) to the instantaneous conductance (I/V) in a PV system. Based on this comparison results, the algorithm increases or decreases the voltage until the maximum power point is reached. Unlike the P&O algorithm, the voltage remains constant once MPP is reached. Algorithm shown in figure 10.

Finally, fractional open-circuit voltage is an algorithm based on the principle that the maximum power point voltage is always a constant fraction of the open circuit voltage. The open circuit voltage of the cells in the photovoltaic cluster is estimated and utilized as in input to the regulator.

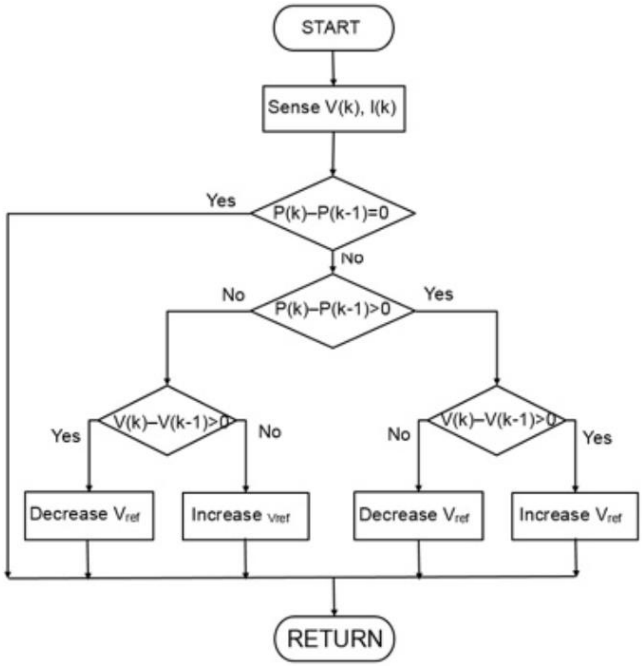

Figure 9. Basic P&O algorithm.

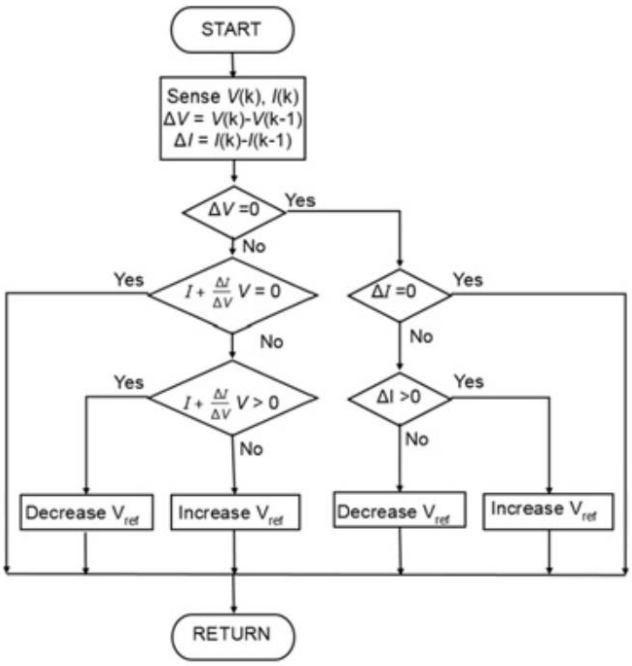

Figure 10. Incremental conductance algorithm.

F. Types of PV Systems

Photovoltaic power structures are overall gathered by their functional and operational necessities, their section plans, and how the rigging is related with other energy sources and electrical loads. The two head groupings are grid-tied or utility-intuitive systems and independent standalone structures. Photovoltaic systems can be proposed to give DC just as AC power organization, can work interconnected with or independent of the utility gird, and can be related with other energy sources and power accumulating structures.

G. Grid tied PV Systems

Grid-tied, on-grid, utility-interactive, grid intertie and grid back feeding are all terms used to define the same concept – a PV system that is connected to the utility power grid.

Grid tied PV structures are expected to work in corresponding with and interconnected with the electric utility grid. The fundamental component in network related PV structures is the inverter, or Power Computing Unit (PCU). The inverter/PCU converts the DC power produced by the PV array into AC control comparable with the voltage and energy quality essentials of the utility

grid, and normally stops giving capacity to the framework when the utility grid network isn't fortified.

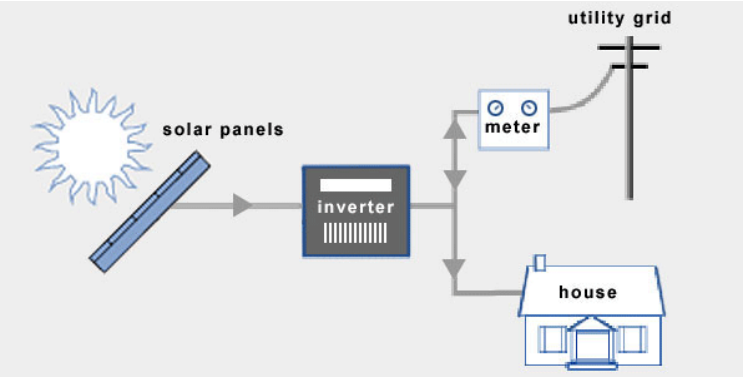

Figure 11. Grid tied PV system

The grid tied PV systems have many advantages such as:

- Cost saving:

Solar panels will usually generate more power than a household is capable of consuming. With many utility companies that are willing to buy electric energy from home owners for the same price they are selling it with, net metering allows homeowners to put excess of electric energy production onto the utility grid instead of storing it into batteries.

- The utility grid is a virtual battery

Although we must consume electricity in real time, we can store in a chemical form knows as batteries and that comes with huge losses.

With the no need for maintenance nor replacement and with better efficiency rates, the utility gird is in many ways seen as a battery. This way, the grid a battery that guarantees more energy with less costs.

Extra advantages of being network tied incorporate admittance to backup power from the utility framework (on the off chance that your PV system quit producing power for some reason). Simultaneously you help to alleviate the utility company's pinnacle load. Thus, the overall proficiency of the electrical framework goes up.

The grid tied PV system is relies on the grid-tie inverter or micro inverter, and power meter as essential components.

As explained in previous section the inverter is a device that changes the nature of a DC voltage into an AC voltage. And power meter or what is often called a net meter or a two-way meter, is a device that measures power going in both directions, from the grid to the house and vice versa.

H. Off-Grid PV Systems

An off-grid solar system (off-the-grid, standalone) is the conspicuous option in contrast to one that is grid tied. Which usually not an option considered by homeowners that have access to the grid.

To guarantee access to power consistently, off-grid network requires battery storage and an emergency backup generator (on the off chance that you live off-the-grid). Besides, a battery bank normally should be supplanted following 10 years. As well as the fact that batteries are confounded, costly and decline the overall framework proficiency.

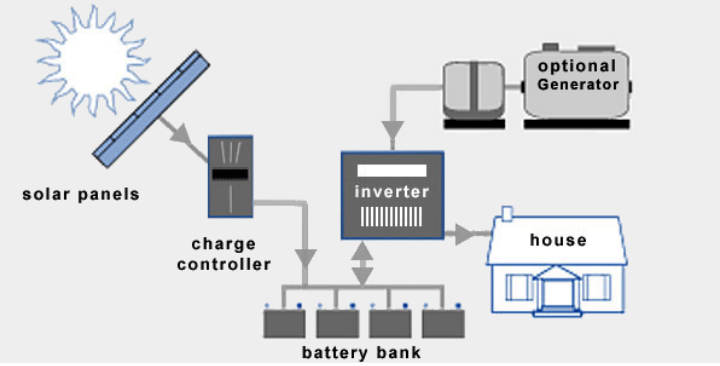

Figure 12. Grid Tied PV System

The off grid has many advantages as well, these advantages include the following:

- Off-grid solar systems can be less expensive than broadening power lines range in certain remote areas.
- Living off the grid and acting naturally adequate feels better. For certain individuals, this inclination feeling is worth more than setting aside cash. Energy independence is additionally a type of security. Power failure on the utility grid don't influence off-grid solar systems.

Typical off-grid solar systems require the following extra components:

- Solar Charge Controller
- Battery Bank
- DC Disconnect (additional)
- Off-Grid Inverter
- Backup Generator (optional)

Solar charge controllers are otherwise called charge Regulators or just battery controllers. The last term is most likely the best to portray what this gadget really does: Solar battery chargers limit the pace of current being conveyed to the battery bank and shield the batteries from overcharging. Good charge regulators are important for keeping the batteries sound, which guarantees that the lifetime of a battery bank is amplified.

The battery bank ensures that the lights will stay on post sundown. We shall explain it more in the following section.

AC and DC safety separate switches are required for all PV systems. For off-grids networks, one extra DC detach is introduced between the battery bank and the off-grid inverter. It is utilized to turn off the current streaming between these parts. This is significant for upkeep, troubleshooting and insurance against electrical fire.

It takes a ton of cash and enormous batteries to plan for a few sequential days without the sun sparkling (or admittance to the grid). This is where backup generators come in.

İ. Hybrid Solar Systems

Hybrid solar systems combines the best from grid-tied and off-grid solar systems. These systems can either be depicted as off-grid solar based with utility reinforcement power, or grid tied solar systems with additional battery stockpiling.

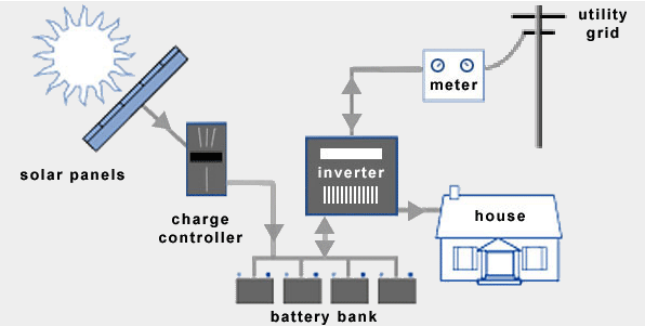

Figure 13. Hybrid Solar System

To mention some of the advantages of the hybrid system, hybrid PV systems are more affordable than off-grid ones. You don't generally require a backup generator, and the limit of your battery bank can be scaled down. Off-peak electric power from the utility company is less expensive than diesel.

The introduction of hybrid solar systems has opened up for many intriguing developments. New inverters let homeowners exploit changes in the utility power rates for the duration of the day. Solar panels happen to yield the most electrical force around early afternoon – not well before the cost of power tops. Your home or electrical vehicle can be customized to consume power during off-top hours (or from the solar panels). Subsequently, we can briefly store whatever overabundance power the solar panels produce in batteries and put it on the utility lattice when you are paid the most for each kWh. Smart PV systems holds a ton of promise. The idea will turn out to be progressively significant as we change towards the smart grid in the coming years more.

J. Batteries and Storage Importance in PV Systems

Batteries are frequently utilized in PV Systems to store power delivered by the PV cluster during the day, and to supply it to electrical loads as required (during the night and times of cloudy weather). Some of the different reasons the batteries are utilized in PV frameworks are to work the PV array close to maximum power point, to control electrical loads at stable voltages, and to supply flood flows to electrical loads and inverters. Much of the time, a battery charge controller is utilized in these systems to shield the battery from overcharge and over discharge.

III. SOLAR INVERTERS

A. Introduction and Definition

Recently as solar PV systems has come to the fore, there is a great interest in inverters today than there ever was. In almost all PV systems, it is the central component that binds the whole system together. Therefore, having a high reliability of an inverter is paramount as it is the component that is most likely to fail other than the batteries. The functionality of an inverter is much higher today than what it was 10 years ago.

The main function of an inverter is to convert DC current to AC current. As the come in all shapes and sizes, inverters are mainly classified based on their power rating or their throughput. For instance, there are small inverters that can convert the output from a car battery to run an AC appliance, as well as there are other inverters that larger and bigger that can convert the out put from a whole solar farm.

There domestic inverters intended to be used by regular consumers, these inverters are available with power ratings ranging from 500W to 10KW.

In a similar fashion, inverters are also classified based on the input that they can accept, meaning they can accept 12V DC, 24V DC, 48V DC, and 96V DC. Note that the 48V DC input inverter is the most common type of inverter that is used for residential solar PV systems, while the 12V DC input inverters are commonly used for portable applications. With that being said, Power inverters in solar farms can also have Maximum input voltages from 300V DC to 450V DC.

B. Why do We Need Solar Inverters?

Apart from the conversion from DC to AC power, Modern inverters have other functions like controlling the solar generator, measurement of AC or DC parameters, measurements, monitoring and protecting the whole solar power system, communication to user or grid. Long story short, today's solar inverters are no less than a high-tech product regarding all its functions. To put in perspective, the internal micro processors' is as powerful as a modern laptop.

C. Off-Grid and Grid Tied Inverter

An off-grid inverter is an inverter that works completely isolated from the grid, it has no provision to tap into the grid electricity or feed electricity to the grid. Normally, if a PV system is designed with an off-grid inverter, then the panels are connected to charge controller that is connected to the batteries, and then the batteries are connected to an off-grid inverter.

Unlike the grid tied inverters, the off-grid inverters can also be made for portable use. Therefore, inverters that are labeled for used in caravans and motorhomes are off-grid converters.

A grid tied inverter on the other hand can be directly connected to the solar array and the grid. There is also sometimes charge control option in the grid tie inverter and therefore, some variants can also be connected to the battery pack. In other words, a grid tie inverter can be the central component of a PV system.

The advantage of a grid tied inverter is that it can feed excess electricity to the grid and take advantage of net metering and can also be used without batteries. Grid tied inverters are more expensive because of such additional functionalities.

Some grid tied inverters have the functionality of shutting down the PV system in case of a power outage. This is done mainly to prevent islanding conditions. These inverters insure that in the event of a blackout, it will shut down the energy being transferred to prevent any harm to the line workers who are sent to fix the power grid.

Grid tied inverters ensure a smooth power feed to the load, which means that they can top-up from either the grid or the battery bank in case the panels are producing enough to meet the load requirements. They can also charge the batteries straight from the grid, provided the grid charger option is inbuilt. This feature proves very useful when the batteries are drained, and the panels are not producing enough energy. And if the panels are over producing, the grid tied inverter can feed this addition energy back to the grid.

D. Pure Sine Wave and Modified Sine Wave inverters

An inverter can produce two kinds of outputs, a pure Sine wave and a modified Sine wave. The modified sine wave inverters are much cheaper than pure since wave inverters since they have less circuitry. The modified sine wave inverters use transistors that acts as a switch that turn on and off the current to create a staircase pulse or a square wave.

Appliances that use a modified sine wave output tend to overuse power and run hotter and thus inefficiently. On the other hand, pure sine wave inverters run electrical appliances smoother, with no buss or a hissing sound

E. Low Frequency and High Frequency Inverters

Inverters can also be classified into two other different categories based on the speed of the operation of transistor switches in the commutator circuit, those categories can be named as low frequency inverters and high frequency inverters.

The low frequency inverter has several advantages, but it is more expensive, and because of the massive iron core in its transformer it is also much bigger and very heavy as opposed to the low frequency inverter. Often, difficult loads that require high surge at the start such as motors, compressors or pumps are managed by low frequency very well. Field effect transistors and low frequency inverters can operate cooler in part due to the slower frequency of the switching required to produce AC power.

In a high frequency inverter there almost twice the number of components compared to low frequency converters, nonetheless, they are smaller and lighter due to the absence of a large central transformer. These inverters are not well

equipped to handle industrial loads and therefore, if a large pump, motor, or an air conditioner is required to be run, the low frequency inverter is proven to be the better choice.

High frequency inverters application is suitable for a wide variety of users, they are suitable for tools, battery chargers, small electrical appliances and even EBN computers. They make up the large majority of inverters available in the detail market. They are also available in lower power rate categories such as 300W, 600W, 1000, 1.5KW …etc. as opposed to the low frequency inverters that have power rating levels that is normally within thousands of kilowatts.

F. MPPT and PWM Charge inverters

A solar inverter is different from a normal inverter based on the fact that a solar inverter has a built-in charge controller. Therefore, inverters used in the solar systems also come with either Maximum Power Point Tracker (MPPT) or Pulse Width Modulation (PWM).

The MPPT functionality allows more to be drawn out of the solar panels. This is done by keeping the panel's output close to the maximum power point of the panels. Inverters with MPPT functionality are more expensive compared to the ones with the PWM option. It has been noted experimentally that, overall, MPPT can make the solar energy system more efficient than the PWM by up to 20%.

The PWM inverters on the other hand are a good low-cost solution for small systems only when the solar cell temperature is mortared too high, that is between 45°C and 75°C. PWM inverters prefer unshaded irradiance on the panel and tend to not work efficiently if the panel is shaded.

G. The History of Solar Inverters

Born to a Serbian family in 1856 in Croatia, Nikola Tesla has greatly impacted our modern lifestyle through his inventions. His genius work has given us the radio, the electric generator, fluorescent lighting, alternative current and plenty other technologies that deliver electrical power to our

households including the solar inverter. Without his impeccable work and great discoveries, we wouldn't have the solar inverters today.

Inverters has first appeared in the late 19th century and continued to develop through the middle of the 20th century. The development was sure steady but a little bit slow, not until the year 2000 when the scientist at the Sandia laboratories in Albuquerque, New Mexico, invented the modern inverter, or as they called it "the non-islanding inverter".

Basically, this device would automatically divert or turns off electricity for potential safety hazard and equipment damage. The problem was that if the utility needed to shut down power in a distribution line for repair or any other reason, the line must be completely de-energized. is a must condition in order to guarantee the safety of the line worker or a passerby that could come in contact with the said line.

The "non-islanding inverter" allowed solar power systems to detect the islanding condition in the line and to automatically shut off power production or divert the electricity to the house or business to which it is connected.

H. Basic Inverters Principle

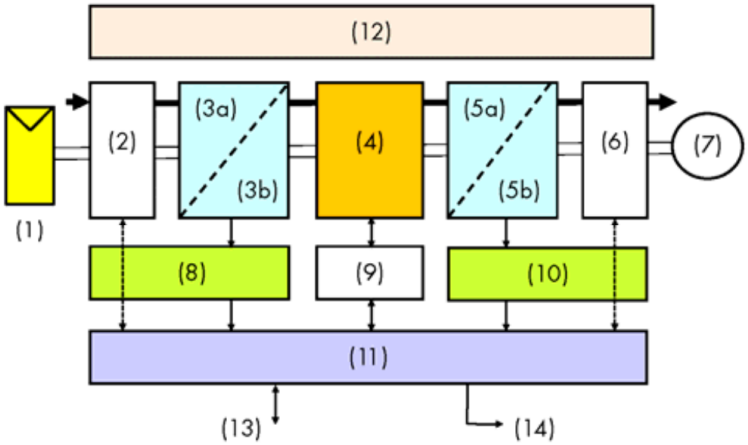

Figure 14. Bloc diagram of a solar inverter

Above in Figure 14, functions of a solar inverter are illustrated in a bloc diagram. Arranged in the best suitable way, the Power semiconductors in bloc (4) constitutes the core of an inverter. Starting from the Solar power generator (e.g. solar cells) bloc (1) we have we have measures for DC protections and

switches in bloc (2), followed by EMI (3a) and DC filter (3b) that sums up the DC side of the inverter.

On the AC side starting from bloc (4), we have A EMI (5a) and a Sinus filter (5b), AC protection and Switches measures in bloc (6) and then finally the utility grid in bloc (7).

We also have the means and equipment for measuring the electrical parameter on both DC and AC side in bloc (8) and bloc (10) respectively. The bloc (9) contains drivers that connects the hardware to the controller unit. as a protection unit, pulse pattern generator we have the controller in bloc (11) that serves also as a controlling, monitoring and interfacing unit. Bloc (12) is a cooler that is connected thermally to all dissipating components such as semiconductors. The cooling unit is connected or integrated to the housing.

İ. Packaging in Solar Inverter Technology

Power Electronic Packaging can be defined as the design and production of the enclosures for any electronic device. It must take into consideration the protection from mechanical damages, cooling, radio frequency noises and electrostatics discharges. Power electronic packaging continuously faces the increasing of the inverter's complexity. In order to add more advantages for user's and grid's advantages, new components are added to the inverter which increases the challenges for the manufacturers as they must integrate these newly added components into the packaging in a simple and fast way [7].

The first generation of solar inverter's concept used a welded pot-type housing of stainless steel, where the aluminum heat sink is attached to the wall bracket with screws. Just as the EMI -filter, inductor and transformer were considered discrete components. They also used discrete semiconductor devices that clipped to a heat transfer block out of aluminum.

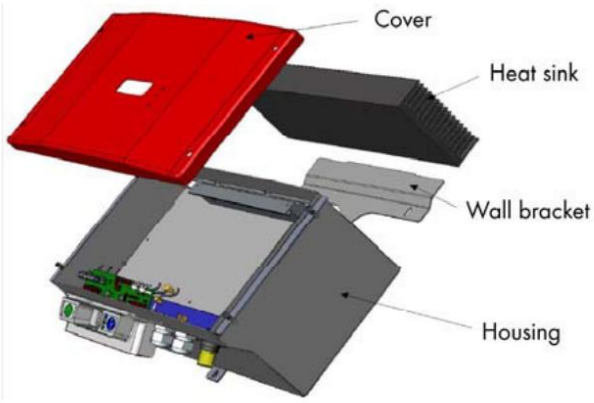

Figure 15. 1st Generation of Inverter

Using a spring type connection in the rear part of the housing, the electrical connection between components, that were installed from bottom to top, was secured. This led to one of the main failure reasons, that is the high number of cable terminal connections.

Driving by the need of a new thermal concept due to the increased power density, the 2nd generation of solar inverter came with an improved thermal management concept that is the 'Opti-cool'.

This cooling concept was devised into two separated compartments. The front compartment (figure 16 a) had the all-sensible electronics components sealed hermetically for installation in outdoor usages while the dissipative components were placed in the vented rear section (figure 16 b).

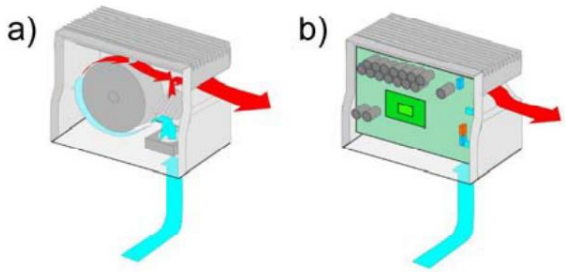

Figure 16. OptiCool® Cooling Concept for Solar Inverters

In figure 17 below we can see the concept of this improved cooling concept based on the Opticool with a front section (figure 17 b) and a vented rear section (figure 17 b). The two fans form two streams of fresh air in and out lead to more cooling power.

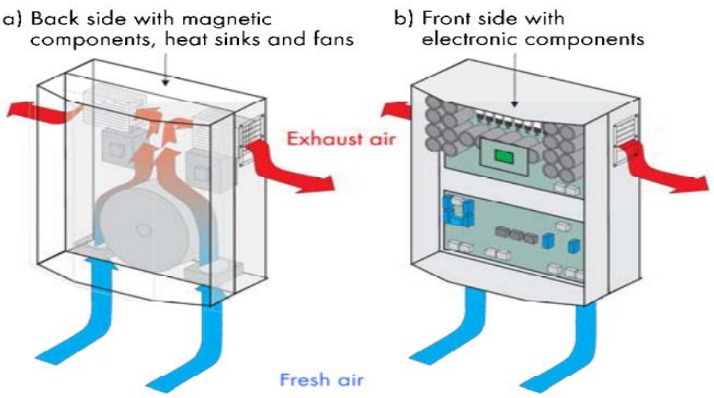

Figure 17. Improved Cooling Concept for Solar Inverters

This also led to better the housing by using the Aluminum die-cast as a housing material. This was the key to integration of several functions in the housing such as the heat sink and grip. The connections between the front and the rear section are achieved via sealed feed-throughs which are screwed to back of the main printed circuit board (PCB), Integrated power module was used instead of the discrete semiconductors and all the EMI-filter components were located on the main PCB in order to decrease the number of cables inside the inverter.

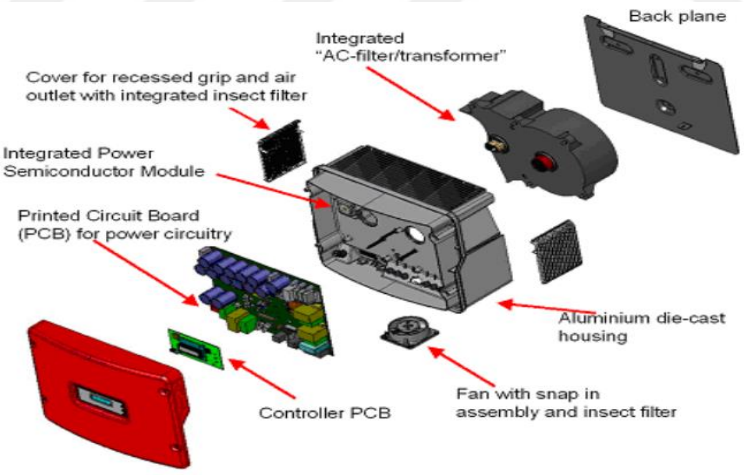

Figure 18. Exploded View of 2nd Generation of Inverters

Which brings us to the third generation that was launched back in 2007. In these inverters, all electronic components were mounted from to the top of the front compartment in order to simplify the manufacturing process. As we see in figure 19 below, the front compartment is divided into three sections, one large and two smaller sections. The large part contains the electronic components inclusive power semiconductor modules. We can find the DC connectors in one

of the smaller sections while the other one has communication devices and Ac connector. The AC and DC connectors' separation provide advantages during regard the safety during the installation, maintenance and service [8].

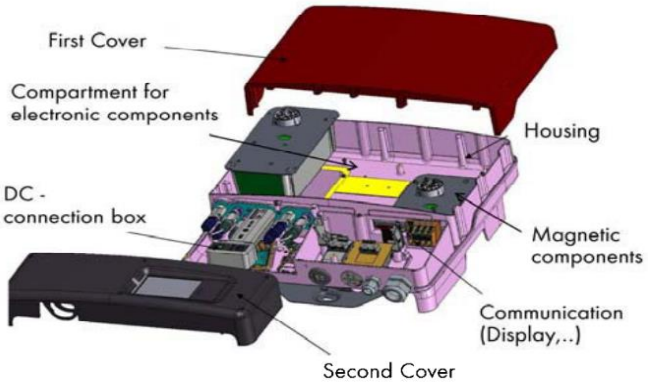

Figure 19. Exploded view of 3rd generation of inverters

J. The Modeling of an Inverter

With the possibility of being of either single phase or three phase output, there are four common grid tied inverters for PV systems: the central plant inverter system, the string inverter system, the multi-string inverter system, and last but not least, the microgrid inverter (AC modules). Being based on centralized inverters that linked with a large number of PV modules to the grid, central plant inverters are considered a passed technology. In order to draw high power levels from the PV modules, we connect them in series into what is called a string, these strings are also connected in parallel with string diodes. String inverters are what we consider modern technology. They are a reduced version of the central plant inverters as each string is connected to its individual inverter, or in case of the multi-string invert where multiple strings are connected to one inverter, which provides the individual controllability that makes them better than the central plant inverters. This brings us to the AC module or the microgrid inverter. It is a small version of a string inverter, where each PV module has its own integrated power electronic interface to the grid [9]. In general, these inverters are used based on their power ratings, where the central plant inverter is used in 1 to5KW, string inverters in 0.5 to 1kW and the AC modules in 0.1 to 0.5KW [10]. Bidirectional operation, highly efficient power converters, measuring and controlling power flows using smart meters and

communication, synchronization abilities, electromagnetic interference filtering (EMI-Filtering) are all a must have feature in the inverters that used in smart grids. The figure 20 displays an inverters bloc diagram.

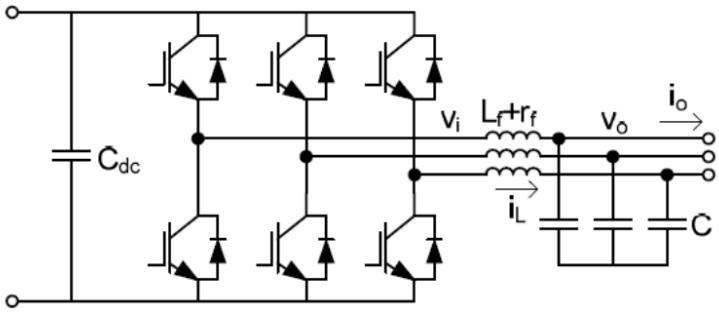

Figure 20. Block Diagram of Three Phase Inverter.

Using the 11 steps below, we can explain the reference output voltage generation [11].

- We start off by obtaining the PLL phase angle using a three-phase output voltage as shown in the flow chart below (fig#). Since the time for each cycle is different, when two signals have different frequencies, it is found that the difference between them is never the same. Therefore, they are moving around in the circle at a different rate.

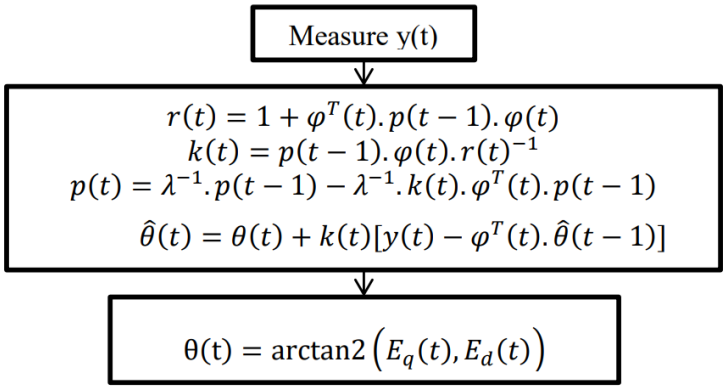

Figure 21. Flow Chart of PLL Phase Angle Generation.

- Clarke conversion for phase voltage

$$\begin{bmatrix} v_{\alpha,in} \\ v_{\beta,in} \end{bmatrix} = \frac{2}{3} \cdot \begin{bmatrix} 1 & \frac{1}{2} & -\frac{1}{2} \\ 0 & \frac{\sqrt{3}}{2} & -\frac{\sqrt{3}}{2} \\ \frac{1}{2} & \frac{1}{2} & \frac{1}{2} \end{bmatrix} \cdot \begin{bmatrix} v_{phaseR,in} \\ v_{phaseS,in} \\ v_{phaseT,in} \end{bmatrix}$$

Equation 9

- Clarke conversion for angle calculation

$$\begin{bmatrix} v_{\alpha,PLL} \\ v_{\beta,PLL} \end{bmatrix} = \frac{2}{3} \cdot \begin{bmatrix} 1 & \frac{1}{2} & -\frac{1}{2} \\ 0 & \frac{\sqrt{3}}{2} & -\frac{\sqrt{3}}{2} \\ \frac{1}{2} & \frac{1}{2} & \frac{1}{2} \end{bmatrix} \cdot \begin{bmatrix} RPLLE \\ SPLLE \\ TPLLE \end{bmatrix}$$

Equation 10

- Clarke conversion for phase current

$$\begin{bmatrix} i_{\alpha} \\ i_{\beta} \end{bmatrix} = \frac{2}{3} \cdot \begin{bmatrix} 1 & \frac{1}{2} & -\frac{1}{2} \\ 0 & \frac{\sqrt{3}}{2} & -\frac{\sqrt{3}}{2} \\ \frac{1}{2} & \frac{1}{2} & \frac{1}{2} \end{bmatrix} \cdot \begin{bmatrix} i_{phaseR,in} \\ i_{phaseS,in} \\ i_{phaseT,in} \end{bmatrix}$$

Equation 11

- Park transformation for voltage and current

$$\begin{bmatrix} v_{d,meas} \\ v_{q,meas} \end{bmatrix} = \begin{bmatrix} \sin(PLLteta) & -\cos(PLLteta) \\ \cos(PLLteta) & \sin(PLLteta) \end{bmatrix} \cdot \begin{bmatrix} v_{\alpha,in} \\ v_{\beta,in} \end{bmatrix}$$

Equation 12

$$\begin{bmatrix} i_{d,meas} \\ i_{q,meas} \end{bmatrix} = \begin{bmatrix} \sin(PLLteta) & -\cos(PLLteta) \\ \cos(PLLteta) & \sin(PLLteta) \end{bmatrix} \cdot \begin{bmatrix} i_{\alpha} \\ i_{\beta} \end{bmatrix}$$

Equation 13

- Reference id and iq calculation

$$v_{dc\_err} = v_{dcbus\_meas} - v_{dcbus\_re}$$

Equation 14

$$i_{d,ref} = K_p . v_{dc\_err} + \int K_i . v_{dc\_err}$$

Equation 15

$$i_{q,ef} = 0$$

Equation 16

- Reference vd and vq calculation

$$v_{D\_err} = i_{d,ref} - i_{d,meas}$$

Equation 17

$$v_{d,ref} = K_p . v_{D\_err} + \int K_i . v_{D\_err}$$

Equation 18

$$v_{Q\_err} = i_{q,ref} - i_{q,meas}$$

Equation 19

$$v_{q,ref} = K_p.\ v_{Q\_err} + \int K_i\ .\ v_{Q\_er}$$

Equation 20

- Current Regulator Feed Forward Value Calculation

$$v_{dFeFo} = v_{d,meas} + (i_{d,ref}.\ R) - (i_{q,ref}.\ L)$$

Equation 21

$$v_{qFeFo} = v_{q,meas} + (i_{d,ref}.\ L) + (i_{q,ref}.\ R)$$

Equation 22

- Converter Reference dq axis calculation

$$v_{dConRef} = v_{d,ref} + v_{dFeFo}$$

Equation 23

$$v_{qConRef} = v_{q,ef} + v_{qFeFo}$$

Equation 24

- Reference U, V, W signal calculation and inverter pulse generation

$$m = \frac{v_{dcbus\_ref}/2}{v_{trf\_sec}.\sqrt{\frac{2}{3}}}$$
$$Re[v_{ConRef}] = v_{dConRef}/m$$
$$Im[v_{ConRef}] = \frac{v_{qConRef}}{m}$$
$$Mag[v_{ConRef}] = \sqrt{Re[v_{ConRef}]^2 + Im[v_{ConRef}]^2}$$
$$Ang[v_{ConRef}] = arctan2(Re[v_{ConRef}], Im[v_{ConRef}])$$
$$Ang_{LegU} = Ang[v_{ConRef}] + 0 + PLLteta - \frac{\pi}{6} + (T_s.f.2\pi)$$
$$Ang_{LegV} = Ang[v_{ConRef}] - \frac{2\pi}{3} + PLLteta - \frac{\pi}{6} + (T_s.f.2\pi)$$
$$Ang_{LegW} = Ang[v_{ConRef}] + \frac{2\pi}{3} + PLLteta - \frac{\pi}{6} + (T_s.f.2\pi)$$
$$Ref_{LegU} = Mag[v_{ConRef}] + \sin(Ang_{LegU})$$
$$Ref_{LegV} = Mag[v_{ConRef}] + \sin(Ang_{LegV})$$
$$Ref_{LegW} = Mag[v_{ConRef}] + \sin(Ang_{LegW})$$

Equation 25

- Finally, we can produce a PWM generation according to Ref_{LegU}, Ref_{LegV}, and Ref_{LegW}.

IV. ONE CYCLE CONTROL SCHEME

A. One Cycle Control Concept

Let's suppose a simple buck converter she in figure 22 below with characteristic as follow:

- Vg is DC source voltage
- The Switch S is operated with a constant frequency of fs=1/Ts
- The diode-Voltage Vs = Vg the power source voltage when the transistor is on and the diode is off
- Vs = 0 when the diode is on and the transistor is off.

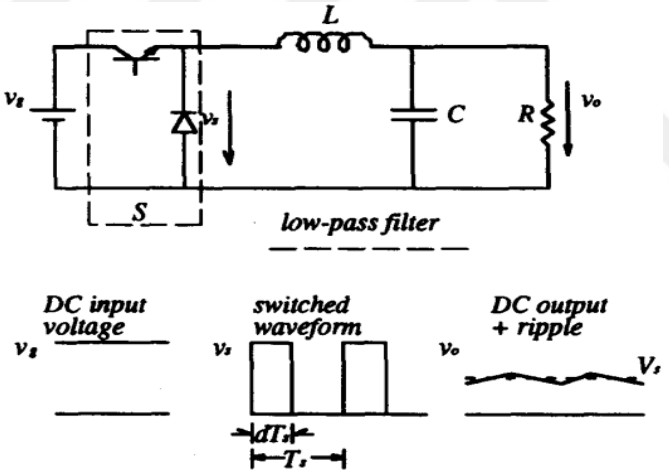

Figure 22. The Buck Converter

This control concept shall be presented on the said buck converter as an example. The control scheme is generalized to control a switch for any type and form signals.

The switched variable Vs is a result of the power source voltage being chopped by the switch. While rejecting most of the unwanted switching frequency components, the LC lowpass filter transmits the average of the switched variable Vs to the output giving us eventually the desired DC value dv_g and a small residual switching ripple at the output voltage.

The idea was provoked by a close observation of the switched variable triggering a new control scheme for constant switching frequency converters shown in figure 23. The observation proved the fact that the output voltage is of the buck converter is the average value of the switched variable, which meant that the diode voltage equals the area under each of the diode voltage pulses divided by the switching period.

$$V_s = \frac{1}{T_s}\int_0^{T_s} v_s\, dt = \frac{1}{T_s}\int_0^{dT_s} v_g\, dt.$$

Equation 26

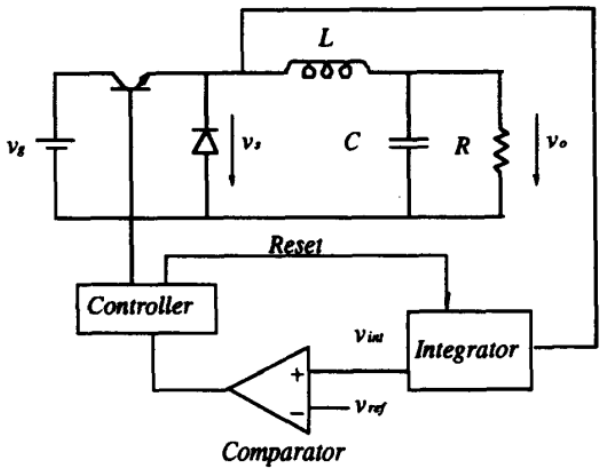

Figure 23. One-Cycle Control of Buck Converter

Coming back to figure 23, at the beginning of each switching period, a constant frequency clock tuns on the transistor. The diode voltage is integrated and then compared to a control reference until it reaches the control reference, and then the comparator changes its state immediately. consequently, the transistor is turned off and the integrator is reset to zero.

If the control reference is a function of time, then the average of the diode voltage us equal to the time variant control reference in each cycle.

Using this control scheme, we can determine the duty-ratio d by:

$$\frac{1}{T_s}\int_0^{dT_s} v_g\, dt = v_{\mathrm{ref}}.$$

Equation 27

Since the duty-ratio d of the current switching cycle being independent of the previous switching cycle state lead, the diode voltage that is the transient of the average value of the switched variable, is completed within one switch cycle.

This nonlinear switch control scheme is called the One-Cycle control [12].

The duty-ratio in the equation (27) presents a nonlinear function of the source power voltage and the control reference. Using the nonlinear control, makes the output voltage of the buck converter a linear function of the control reference that is independent of the power source voltage

$$v_o = \frac{v_{\text{ref}}}{1 + \frac{L}{R}S + LCS^2}.$$

Equation 28

B. One Cycle Control Theory

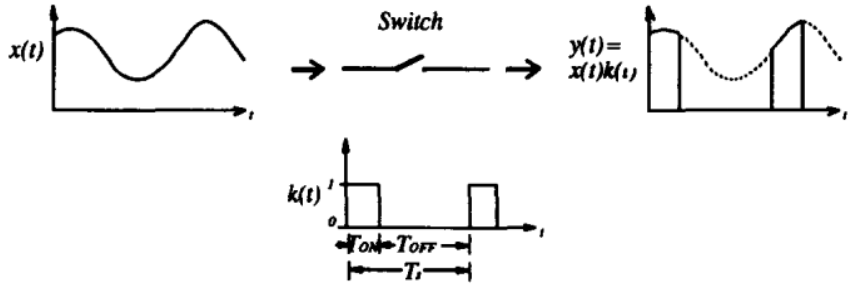

Figure 24. The Switch Function

Suppose we have the switch function k(t) shown in figure 24 where the switch operates according to at frequency of fs = 1/Ts.

$$k(t) = \begin{cases} 1 & 0 < t < T_{\text{ON}} \\ 0 & T_{\text{ON}} < t < T_s. \end{cases}$$

Equation 29

As shown in figure 24 above, the switch is on for a time period TON and off for a time period T_{OFF} where $T_{ON}+T_{OFF}=T_s$. We have the analog control $V_{ref}(t)$ that modulates the duty ratio is $d=T_{on}/T_S$, and the variable y(t) that is defined as

the signal obtained by chopping the input signal x(t) by the switch and transferred to the output nod of the switch. k(t) and y(t) have the same frequency and pulse width, while the envelope of the switched variable y(t) is the same as the input signal x(t):

$$y(t) = k(t)x(t)$$

Equation 30

Suppose the switch frequency f_s is much higher than the bandwidth of x(t) the input signal or $V_{ref}(t)$ the control reference, then the effective output signal is:

$$\begin{aligned} y(t) &= \frac{1}{T_s}\int_0^{T_{ON}} x(t)\ dt \\ &\approx x(t)\frac{1}{T_s}\int_0^{T_{ON}} dt \\ &= x(t)d(t). \end{aligned}$$

Equation 31

We can conclude that the output signal y(t) is the product of the input signal x(t) and the duty ratio d(t), therefore, the switch is nonlinear.

If we can regulate the duty ratio so that the integration switched variable at the output is equal to that of the control reference in each cycle, meaning that

$$\int_0^{T_{ON}} x(t)\ dt = \int_0^{T_s} v_{\mathbf{ref}}(t)\ dt$$

Equation 32

And since the switching period is always constant, the average value of the output is equal to the control reference in each cycle. Therefore, the average of the switched variable is instantaneously controlled within one cycle, meaning that

$$\begin{aligned} y(t) &= \frac{1}{T_s}\int_0^{T_{ON}} x(t)\ dt \\ &= \frac{1}{T_s}\int_0^{T_s} v_{\mathbf{ref}}(t)\ dt = v_{\mathbf{ref}}(t). \end{aligned}$$

Equation 33

As we could guess by now, this control technique that is based on controlling switches according to this concept is called One Cycle Control technique. This technique ensures that the effective output signal of the switch is

$$y(t) = v_{\mathbf{ref}}(t).$$

Equation 34

The one cycle control scheme turns a nonlinear switch into a linear path, since the switch fully reject the input signal all-pass the control reference $V_{ref.}$

The key component of the OCC is the integrator and the resetter. When the switch is turned ON by the fixed frequency clock pulse, the integration starts immediately. The integration value,

$$v_{\text{int}} = k \int_0^t x(t)\, dt$$

Equation 35

is compared with the control reference $V_{ref}(t)$ instantaneously where K is constant. Once the integration value V_{int} reaches the control reference $V_{ref}(t)$, the controller turns OFF the switch and resets integrator to zero at the same time. This can be seen and explained in the implementation circuit of OCC led constant-frequency switch shown in the figure 25 below

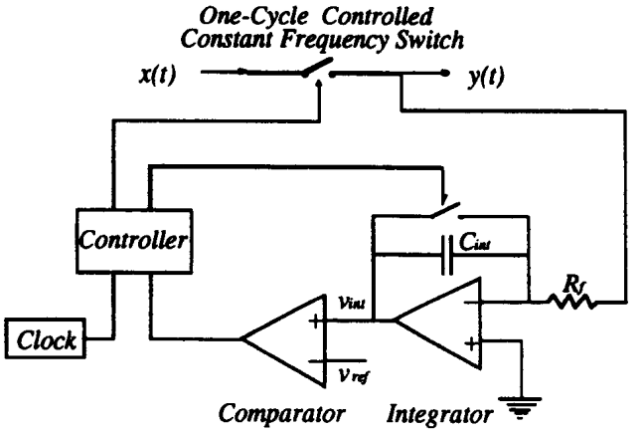

Figure 25. The One-Cycle Controlled Constant Frequency Switch.

The duty ratio $d = T_{ON}/T_s$ of the present cycle can be determined by the following equation

$$k \int_0^{dT_s} x(t)\, dt = v_{\text{ref}}(t)$$

Equation 36

Knowing that the switch period T_s and the $K=1/kT_s$ are both constant, we can conclude that the average value of the output switched variable y(t) in each cycle is undoubtedly

$$y(t) = \frac{1}{T_s} \int_0^{dT_s} x(t)\, dt = K v_{\text{ref}}(t)$$

Equation 37

C. Modeling an OCC Three Phase Inverter

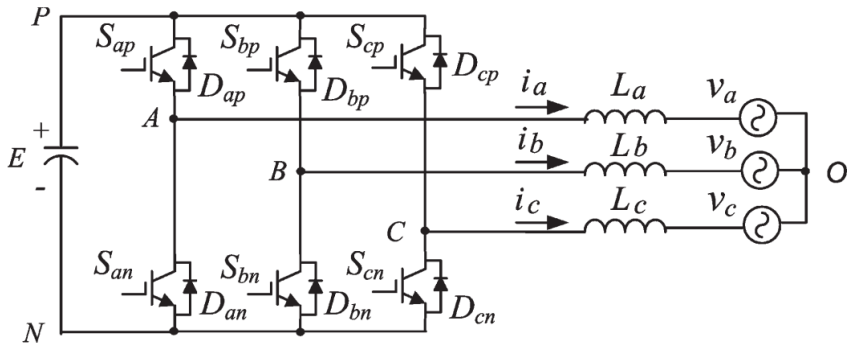

Figure 26. Three-Phase Grid-Connected Inverters.

In figure 26 we can see the typical six-switch bridge topology of three-phase grid tied inverter. In this figure we have:

- The DC source voltage is represented by the symbol E
- v_a, v_b, v_c represent grid voltages

Suppose that the switching frequency is much higher than the line frequency, the bridge is the same as three voltage-controlled- sources and its equivalent switching-cycle average model can be derived as shown in figure 27 below.

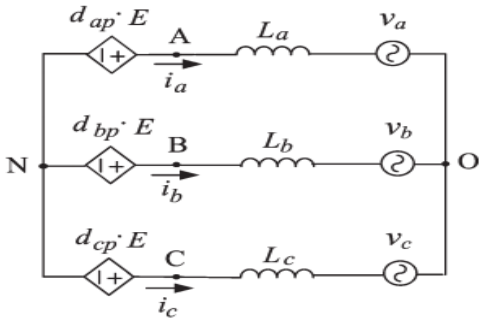

Figure 27. Switching-Cycle Average Model

In the figure above, d_{ap}, d_{bp}, and d_{cp}, are duty ratios for S_{ap}, S_{bp}, and S_{cp} respectively. The point-by-point study concludes that the relationship of the input and the output voltages:

$$\begin{bmatrix} \frac{2}{3} & -\frac{1}{3} & -\frac{1}{3} \\ -\frac{1}{3} & \frac{2}{3} & -\frac{1}{3} \\ -\frac{1}{3} & -\frac{1}{3} & \frac{2}{3} \end{bmatrix} \cdot \begin{bmatrix} d_{ap} \\ d_{bp} \\ d_{cp} \end{bmatrix} = \frac{1}{E} \cdot \begin{bmatrix} v_a \\ v_b \\ v_c \end{bmatrix}$$

Equation 38

Knowing that the matrix on the left side of the equation (38) is singular, the equation has no unique solution. Which means that there are two methods of to implement the OCC method in an inverter, the Bipolar mode and vector operation mode.

- OCC Inverter with Bipolar Operation Mode

We can generate duty ratios by sensing and controlling all three-phase currents. In this case, the switches are controlled with switching frequency to regulate the current and track each phase voltage tightly, this provides us with a practical solution for equation (39)

$$\begin{cases} d_{ap} = K_3 + \frac{v_a}{E} \\ d_{bp} = K_3 + \frac{v_b}{E} \\ d_{cp} = K_3 + \frac{v_c}{E} \end{cases}$$

Equation 39

Keeping the output currents sinusoidally and in-phase with the grid voltages is the main control goal for a three-phase inverter with unity power-factor. Consequently, by subbing the control purpose $V_j = R_e \cdot i_j$ (j = a, b, c) into the equation (40), the following control key equation can be obtained

$$\begin{cases} K v_a - R_s . i_a = V_m \left(\frac{d_{ap}}{K_3} - 1 \right) \\ K v_b - R_s . i_b = V_m \left(\frac{d_{ap}}{K_3} - 1 \right) \\ K v_c - R_s . i_c = V_m \left(\frac{d_{ap}}{K_3} - 1 \right) \end{cases}$$

Equation 40

Where K and V_m are considered as constant and the real value of phase current and determine the upper boundary respectively. Rs is current sensing resistance while K3 was conveniently chosen to be 0.5. the implementation of the OCC circuit is shown in figure 28 below. In order to create the duty ratios in each switching cycle for all switches, three-phase currents are provided to the controller which leads each current to follow its corresponding voltage strongly.

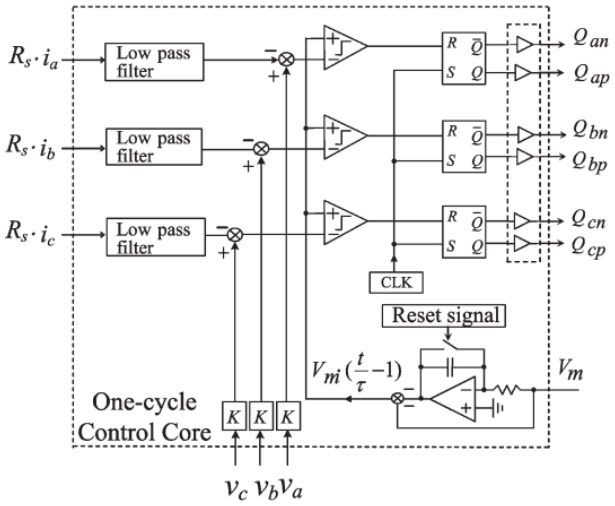

Figure 28. OCC Controller with Bipolar Operation Mode.

As for the OCC Inverter with Vector Operation Mode, a brief explanation can be found in [13] and a more profound dive through can be found in [14].

V. MICROGRIDS

A. Definition and Purpose

With 60% of the human population set to be living in urban areas by 2030 - and pressure on regional and national power grids continuing to grow - a number of cities are now turning towards localized energy production for new developments.

As the name suggests, “Microgrids” are small scale electrical networks that operate independently, or in tandem with, large scale electrical supplies. While many national and regional electrical grids are now powered in part by renewable energy, the majority still depend on nuclear and fossil fuels to deliver the bulk of their power.

Inversely, microgrids make heavy use of renewables such as photovoltaics and wind turbines to generate energy for use within a specific building or development. This enables them to power their systems and operate without adding to the demands of the wider electrical network. On-site energy production and storage can enable a new development to become self-sufficient and helps to fill in the gaps that can arise on overstretched electrical grids.

As part of their pledge to honor the 2016 Paris Agreement on climate change, cities around the world are passing legislation to make all new public buildings and developments emission free. The use of microgrids can contribute significantly to achieving these requirements whilst better Excess energy generated on small scale systems can be stored on site for use at a later date or be fed back into wider power grids when necessary.

Whilst legislation is one step, private enterprise is also getting onboard with microgrids and localized energy production. Pursuing clear environmental benefits and reduced operating costs, to integrate systems from forward-thinking manufacturers and technology entrepreneurs alike. One such manufacturer is Polysolar - a UK based firm who have developed transparent

photovoltaic glass. Their panels can be used to cover large areas without obstructing views and resemble conventional windows. Though currently emerging, this system could be adapted to cover larger glass buildings in cities around the world, allowing them to generate much of their own electricity. On a more domestic scale, Elon Musk's "Tesla Solar Roof" integrates photovoltaics into conventional appearance roof tiles, turning entire surfaces into localized power generators. This system is integrated with the Tesla Power Wall allowing excess energy to be stored and used throughout the year.

Many large- and small-scale developments are also now incorporating wind turbines to generate power and feed their microgrids, reducing their reliance on regional and national power networks. Energy market analysts Pike Research estimate that microgrid power generation has now increased fivefold from 2012 levels - and with an increasing array of innovations coming to market we could see entire cities and urban areas powered very differently in the years ahead.

B. Smart Microgrids

Our current electric grid was conceived more than 100 years ago when electricity needs were simple. Power generation was localized and built around communities. Most homes had only small energy demands such as a few light bulbs and a radio. The grid was designed for utilities to deliver electricity to consumers' homes and then bill them once a month. This limited one-way interaction makes it difficult for the grid to respond to the ever-changing and rising energy demands of the 21st century. The smart grid introduces a two-way dialogue where electricity and information can be exchanged between the utility and its customers. It's a developing network of communications, controls, computers, automation and new technologies and tools working together to make the grid more efficient, more reliable, more secure and greener.

This smart grid enables newer technologies to be integrated such as wind and photovoltaic energy production and plug-in electric vehicle charging with our participation as informed consumers. This smart grid will replace the aging infrastructure of today's grid and utilities can better communicate with us to help manage our electricity needs. The smart home communicates with the grid

and enables consumers to manage their electricity usage. By measuring a home's electricity consumption more frequently through a smart meter, utilities can provide their customer with much better information to manage their electricity bills.

Inside the smart home, a Home Area Network (HAN) connects smart appliances, thermostats and other electric devices to an energy management system. Smart appliances and devices will adjust their run schedule to reduce electricity demand on the grid at critical times and lower consumers energy bills. These smart devices can be controlled and scheduled over the web or even a TV. Renewable resources such as wind and solar are a sustainable and growing source for electric power. However, renewable power sources are variable by nature and add complexity to normal grid operations. The smart grid provides the data and automation needed to enable solar panels and wind farms to put energy onto the grid and optimize its use. To keep up with constantly changing energy demands, utilities must turn power plants on and off depending on the amount of power needed at certain times of the day. The cost to delivered power depends on the time of day it is used; electricity is more costly to deliver at peak times because additional and often less efficient power plants must be run to meet the higher demand. This smart grid will enable utilities to manage and moderate electricity usage with the cooperation of their customers; especially during peak demand times. As a result, utilities will be able to reduce their operating costs by deferring electricity usage away from peak hours and having appliances and devices run at other times. Electricity production is more evenly distributed throughout the day.

The power being used right now was generated less than a second ago many miles away. At each instance the amount of electricity generated must equal the consumption across the entire grid. Smart Grid technologies provide detailed information that enables grid operators to see and manage electricity consumption in real time. This greater insight and control reduce outages and lowers the need for peak power. In control rooms across the grid, engineers will be able to, more precisely and predictably, manage electricity production, reducing the need to fire up costly secondary power plants.

The distribution system routes power from the utility to residential and commercial customers through power lines, switches and transformers. Utilities typically rely on complex power distribution schemes and manual switching to keep power flowing to their customers; any break in this system caused by storms bad weather or sudden changes in electricity demand can lead to outages. The smart grids distribution intelligence counters these energy fluctuations and outages by automatically identifying problems, rerouting and restoring power delivery.

Utilities can further use distribution intelligence to predict and manage electricity usage with the cooperation of their customers, leading to lower production cost.

To summarize, The Smart Grid is a developing network of transmission lines, equipment, controls and new technologies working together to respond immediately to our 21st century demand for electricity.

C. The Used Microgrid Topology Explained [17]

In a microgrid-based smart conveyance network topology, each dc load, generator, or energy stockpiling device is furnished with its DC–AC inverter and associated with the ac microgrid by means of shrewd devices we shall call special control units (SCUs). SCUs are additionally fundamental for the ac loads (or group of loads) and ac generators too, as appeared in Figure 29 [20][21]. The SCUs are ordered in load SCUs (L-SCUs), stockpiling or storage SCUs (S-SCUs), generators SCUs (G-SCUs), and interconnection SCUs (I-SCUs), for interfacing the little grid of the ac-bus to the rest of the grid (SD).

All SCUs comprise of a basic metering module, a correspondence module, an enactment module (actuator), and a "smart" module that is responsible for the dynamic of each SCU. The last module is incorporated into software that runs in demand for a microgrid-committed PC. This topology is actualized at the offices and facilities of the Technological Educational Institute of West Macedonia (TEIWM) and is appeared in Figure 30.

The microgrid comprises of two PV-inverters of 1.1 kW each, with six associated PV panels each, five loads of roughly 2600-W max utilization, a 600-Ah-24-V battery unit with its inverter, and one wind generator of 1 KWp with its rectifier-charger. The whole output intensity of the wind generator is redressed and directed to the battery and afterward the battery power is modified and diverted to the ac bus. Ten SCUs are required: two for the PV plants, five for the loads, one for the battery bank, one for the wind generator, and one for the interconnection to the rest of the grid. Each SCU contains one current transformer (CT), one voltage transformer (VT), and one actuator-relay and communicates with the microgrid-devoted PC by means of links and an information acquisition card (DAQ: NI6008). Be that as it may, because of the normal ac bus, just a single ac VT is required, and one dc VT for the battery bank. The entirety of the metering equipment is adjusted at the Low Frequency Laboratory, Electrical Department, Hellenic Institute of Metrology.

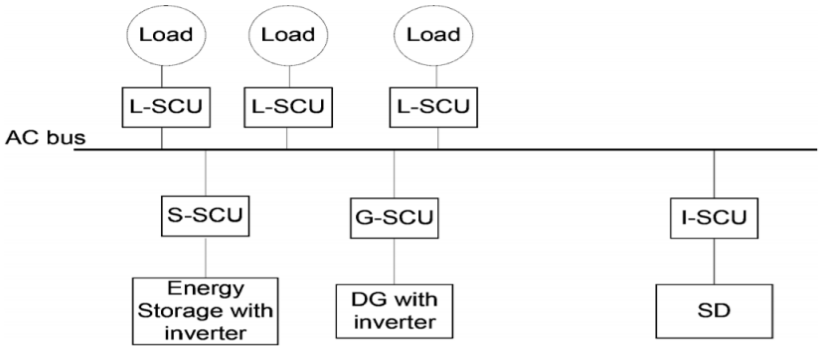

Figure 29. Smart Distribution Grid Topology with SCUs

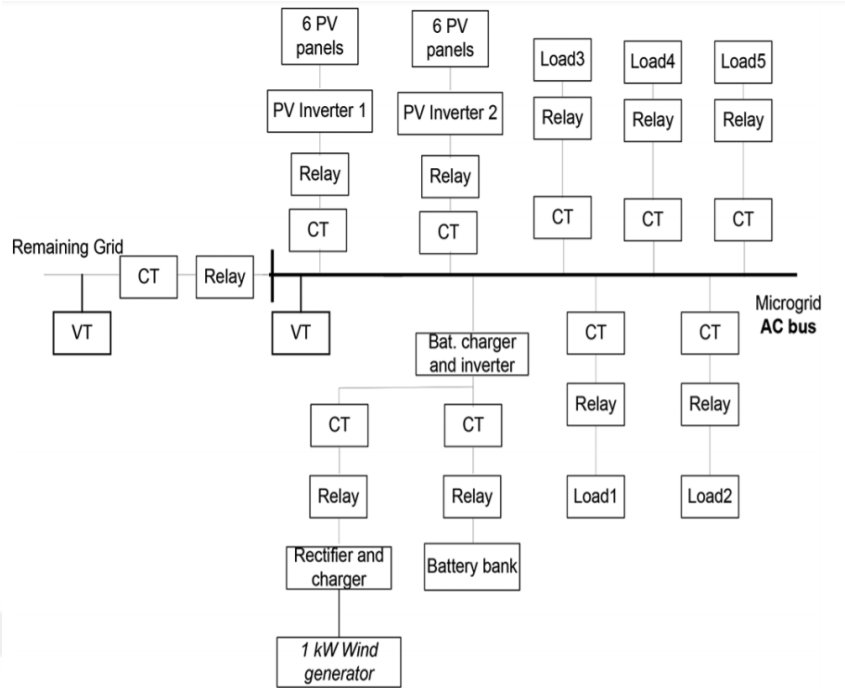

Figure 30. Smart Distribution Gird Topology Incorporated, TEIWM Microgrid.

In order to show the importance of these energy stockpiling and PV active power management schemes, especially while an islanding occurrence, we compare them to different scheme and topology [22] and shown in figures 31 and 33. In figure 32, the island-inverter can switch off the loads automatically when the battery voltage is too low using a load shedding circuit. This circuit has a normally close contact (NC) and installed between the inverter and the loads. The system enters an islanding state when the battery voltage and current falls to 30% or under, the relays are then activated, and all the loads disconnect. Besides, all PV active power control is no longer applicable. The single dc-bus of this topology and the used energy storage management scheme have some severe inconveniences especially during islanding mode. Though the available supply, demand and storage are carefully matched, this topology suffers from constant load switching, quick batteries charging and discharging, inaccurate estimation of the state of charge (SoC) of the batteries and more importantly, a weak renewable energy exploitation.

Because we must build a dc-grid, and this requires a large amount of investment to develop it to the appropriate size, the expansion of the topology in Figure 31 to a larger scale rather difficult and not easy to sponsor.

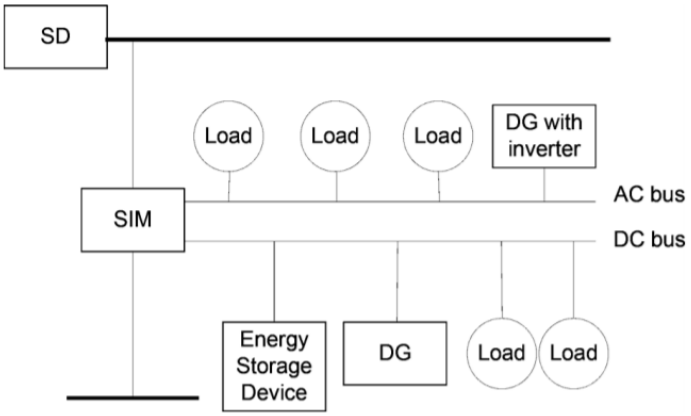

Figure 31. DC Bus-Based Smart Distribution Grid Topology Where SD is the Rest Grid.

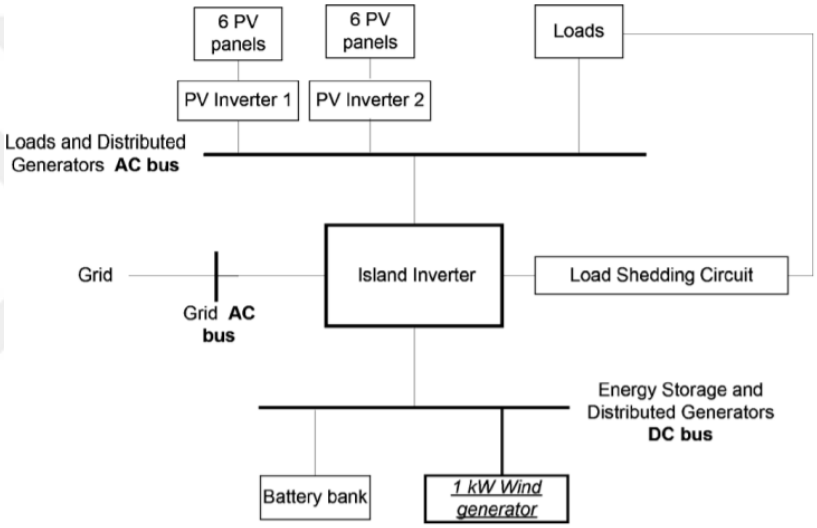

Figure 32. Implementation of the DC bus-based smart grid. The island inverter at the center is the SIM of Figure 31.

It is possible to expand the improved microgrid topology to a larger scale. This can be done if we correct the limitation of the existing system in figures 30 and 31. The presented limitations are as follow:

- Wireless signal transmission to replace the cables
- Synchronization of the grid voltage with the microgrid voltage during transition from the islanded to interconnected operation
- The use of phasor measurements units (pmus)
- Adding weather conditions measurements to the control algorithm

The purpose of 4th correction is to include prediction options by incorporating fuzzy cognitive networks (FCNs) into the control algorithm.

D. Iterative Storage Control Algorithm

At the microgrid-devoted PC, a software application in Labview measures the input data, fuses the control calculation in MATLAB and infers the correct yield orders each obligation cycle.

A Labview application grants us data sampling and conversion to RMS values in each duty-cycle as well as calculating other parameters such as frequency, active and reactive power; integration of the control algorithm in Matlab code; transmission of the orders determined by the control algorithm to the advanced output of the DAQ card and eventually data recording.

Real time measurements are updated in each duty cycle by the mentioned Labview app as well as the output variables that are fed back into the control algorithm at the end of the execution period are incorporated as the inputs of the control algorithm. One of the output factors is the ten initiation modules cluster that is sent to the digital output of one DAQ card. The algorithm is executed in less than 10ms every duty cycle that is obligatory longer than 100ms because of the duration of the data sampling and calculation in the Labview app that hosts the algorithm. The real-time measurements inputs of the algorithm are:

- The arrays of the ac active power and ac reactive power delivered by the PV inverters (Pinv) and (Qinv) respectively that comprises of two values each that are measured in watts and var respectively;
- The array of the ac active power as well as the ac reactive power consumed by the loads (PL) and (QL) that consists of five values each;
- The ac voltage of the microgrid ac bus (Vac);
- The ac active power and ac reactive power produced or consumed by the remaining grid at the interconnection point of the microgrid with the remaining grid (Pinter) and (Qinter);
- The microgrid's frequency in Hz (f);
- The batteries' dc current (Idcsto);
- The batteries' and the wind generator's dc voltage (Vdcsto);
- The wind generator's dc current (Idcw);
- The critical loads vector (crv) which is the vector determining the degree of significance of the loads: it can change with time within the

algorithm or set by the user. It can take values from 1 to 5, where 1 is the most critical and 5 is the less critical load. This vector is used by the algorithm in order to define the load shedding policy of the microgrid.

The algorithm's outputs that are fed back to the algorithm as inputs are:

- The batteries' previous soc;
- The previous activation modules state (rel). These modules consist of a ten values array taking values where 0 is for a relay that should be open and 1 for a relay that should be closed (this array is also transmitted to the digital output of one DAQ card);
- Fault diagnosis of the system assisting group of flags;
- A group of counter and averaging factors that is utilized by the algorithm.

There are two major steps that this algorithm is consisted of:

- The constant voltage and frequency observation and correction, just as the interoperability with the rest of the framework. This aspect of the algorithm is introduced as a block diagram beneath in figure 33.

First Major Step of the Control Algorithm: Real-time voltage and recurrence control. Interoperability with the rest of the grid.

As additionally seen tentatively, in microgrids without rotating generators and with R/X ratio higher than 2 (like the one introduced here), the voltage level relies upon the active power balance [24], [25]. In view of this perception, the diagram presented in Figure 33 is executed in this progression.

- The proposed energy stockpiling management scheme, which comprises of the SoC assessment routine and the particular DGs and load management activities. This aspect of the algorithm is introduced in detail in the following Section 5.5 and 5.6.

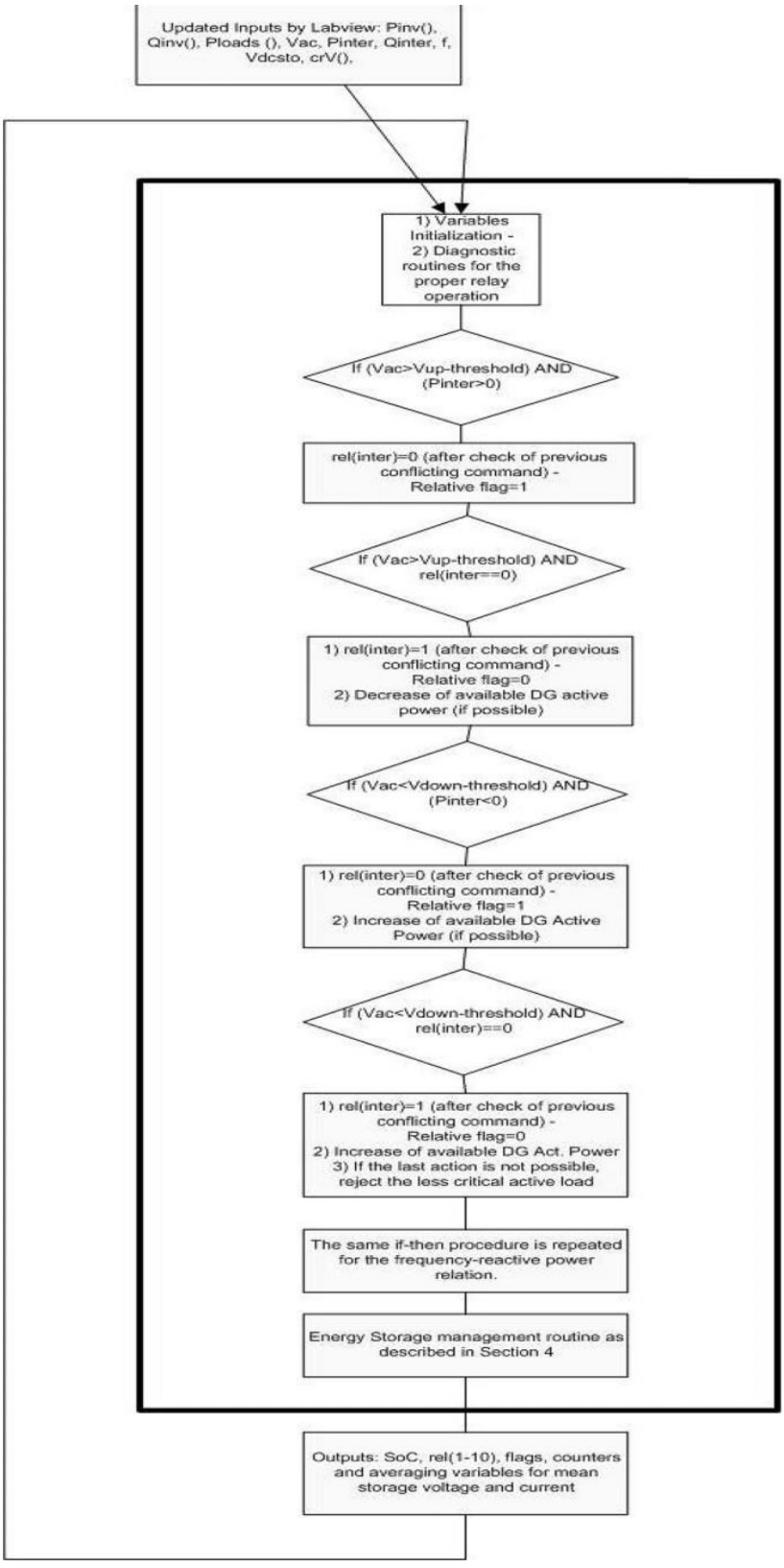

Figure 33. Control Algorithm

E. Strategy of Energy Storage Management [17]

The reliability of the method of the SoC estimation is a essential factor in the success of an energy storage management strategy [20]. The used method must have certain criteria such as accuracy, cost-effectiveness, simplicity, and not to forget, commercial exploitability. To sum up these criteria we can say that the method should be a “plug and play” method. There are few methods to estimate the SoC that has been developed throughout the years, the following listed methods all have other disadvantages, however, the last one fulfills all the criteria mentioned above.

- The electrolyte density measurement method [26] is precise yet costly, and chemical components estimating gear must be accommodated the batteries of the bank.
- The open-circuit method [26] can't be applied for real time estimations.
- The Coup de Fouet method requires full charge of the batteries, which is most never happens in actual framework [28].
- Neural Networks methods [29], [30], [31] that are not commercially exploitable since they require an extensive operation data from the particular battery bank.
- The impedance spectroscopy method [21] has a very high sensitivity to temperature and is quite complex.
- The Ah balance method [26] is accurate enough, however, it requires regular re-calibration points and expensive which renders it hard to commercials.
- The Kalman filter method [29] needs huge processing limit and the assurance of starting boundaries.
- The linear model [26], [27] is straightforward, solid, and suitable for PV uses of batteries, an implementation of this methods can be found in [27].

In order to determine the SoC of the batteries, we continuously measure the dc-bus voltage and current. The current-voltage characteristic curves that is corresponding to different SoC values of the battery are reproduced and then have the normalized measurements of the dc-bus compared to them. After the

proper time delay and voltage-hysteresis are considered, the new SoC is determined from the curves.

The new SoC sparks the following actions:

- If the soc lies above the “soc = 0.4” curve which corresponds to state of charge of 40%, no action is taken
- If the soc lies between the “soc = 0.4” curve and the “soc = 0.3” curve, a warning signal is displayed
- If the soc lies below the “soc = 0.3” curve, all loads are rejected.

However, since other dc-sources are connected to the dc-bus as well, and because the previous SoC as well as the power production of each source and each loads’ consumption are all ignored, this method is deemed inefficient.

In order to improve this method, only the dc voltage and current of the batteries is measured, the previous SoC and DGs power production are taken into account, and more targeted control actions are taken. It is set among the heuristic understanding strategies for estimations curves, along with the Coup de Fouet strategy and the Neural Networks technique.

In summary, during the duty cycle of the LabVIEW app, the batteries voltage and current along with each RES power production as well as each load’s consumption are measured. For independent 2mins, 6mins,15mins, and 30mins periods, the mean batteries voltage per cell and the mean batteries current per 100Ah are calculated ($V_{mean\text{-}m}$, $I_{mean\text{-}m}$, where m=2,6,15,30). The current–voltage characteristic curves of leadacid batteries that correspond to SoC equal to 60% (SoC=0.6), 40%(SoC=0.4) and 25% (SoC=0.25) are reproduced, respectively, in.

$$
\begin{aligned}
&\mathbf{SoC = 60\%}\\
&\quad V = 2.03 - 0.005^{*}I, \qquad \text{for } I > 1\ A\\
&\quad V = 2.06 - 0.035^{*}I, \qquad \text{for } I < 1\ A\\
&\mathbf{SoC = 40\%}\\
&\quad V = 1.995 - 0.005^{*}I, \qquad \text{for } I > 1\ A\\
&\quad V = 2.025 - 0.035^{*}I, \qquad \text{for } I < 1\ A\\
&\mathbf{SoC = 25\%}\\
&\quad V = 1.97 - 0.005^{*}I, \qquad \text{for } I > 1\ A\\
&\quad V = 2 - 0.035^{*}I, \qquad \text{for } I < 1\ A
\end{aligned}
$$

Equation 41

Where V and I are the voltage per battery cell and the battery current respectively which are plotted in figure 34.

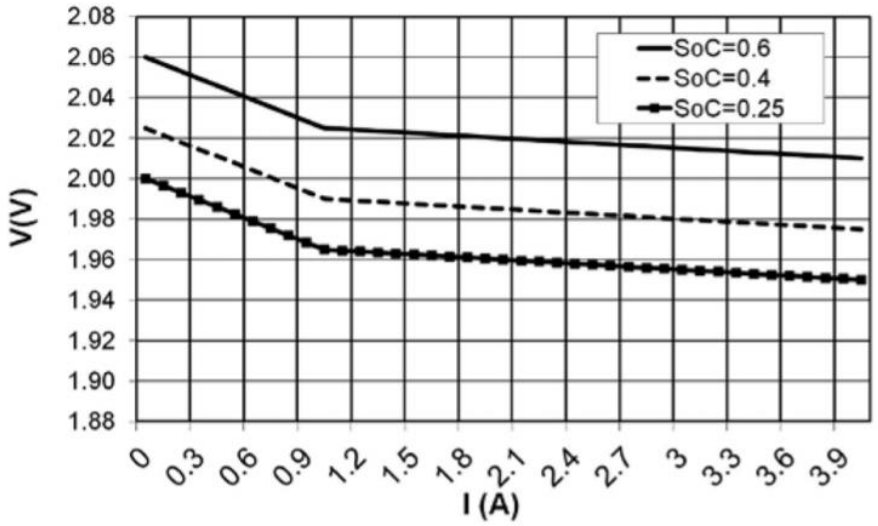

Figure 34. Current–Voltage Characteristic Curves of Lead-Acid Batteries that Correspond to SoC Equal to 60%, 40%, and 25%.

The mean standardized current and voltage values are contrasted with these characteristics curves in order to determine where they fall (e.g above 60% curve, between 60% and 40% curves, under 25%curve... etc). Taking into consideration the previous stare of charge SoC_{i-1}, the actual state of charge SoC_i is calculated. The reason why we are taking the SoC_{i-1} is that a huge discharging currents has been noticed when there's a switching on-off of a large load, which consequently give misleading indications that prevents from correctly estimating the SoC using the linear method. In other words, according to experiments and trails, a significant drop has been noticed in the batteries SoC in a short amount of time, which means a time-hysteresis of 2 means leads to a gradual increase of the SoC, meanwhile rejecting a less critical small load will generate a great increase of the SoC. Therefore, as a result of the inaccuracy of the classical linear method's estimation of the SoC, an unnecessary load rejection is occurred and eventually the power supply reliability is decreased.

To overcome this error, a state of charge is purposefully assigned to the batteries when a great discharging current appears in a 2 min span and point (V_{mean-2}, I_{mean-2}) skips one of the SOC areas in figure 34 (e.g initial SoC = 0.65

and new SoC= 0.3). This assigned SoC shall be called Pseudo-SoC which is the missed area SoC.

When the SoC is determined, the taken DGs and load management actions can be found in[17].

F. The Control Strategy of the PV-Plant Active Power

The PV-Plant control technique comprises of legitimate actuator-relay amalgams that are applied at the PV strings circuits [18]. The number of selected actuators relies upon the PV power that needs to be controlled. An example of the applied control on a typical PV plant is shown in figure 33, where, theoretically, the PV output power can change in the range of 70-100% with 3.3% steps of the PV system's capacity. Obviously, if the actuators are installed at one or three panels, the output power step can be different. Thanks to DC-side capacitors of the PV inverters, the continuous PV power supply is not affected by the interruption of the string circuits during the change of the relays. The one drawback spotted in this strategy is that in real life applications where MPPT option is in operation, the output power step cannot be predicted accurately. However, the iterative nature of the algorithm allows us to overcome this drawback. The relays can be set off based on different patterns, contingent upon the wanted auxiliary service to be provided. The last gathers vitality estimations from the microgrid and decides the ideal PV plant power generation at both significant steps of the control algorithm. The PV control scheme is applied on both PV strings of Figure 30. Since the lower voltage operation cutoff of the PV inverters is 150 V and every last one of the six panels of the string has an open circuit voltage of 37 V, one actuator is introduced at an equivalent number of the six panels of each string. Each relay of the V-strings is set off by the individual digital output of the DAQ cards.

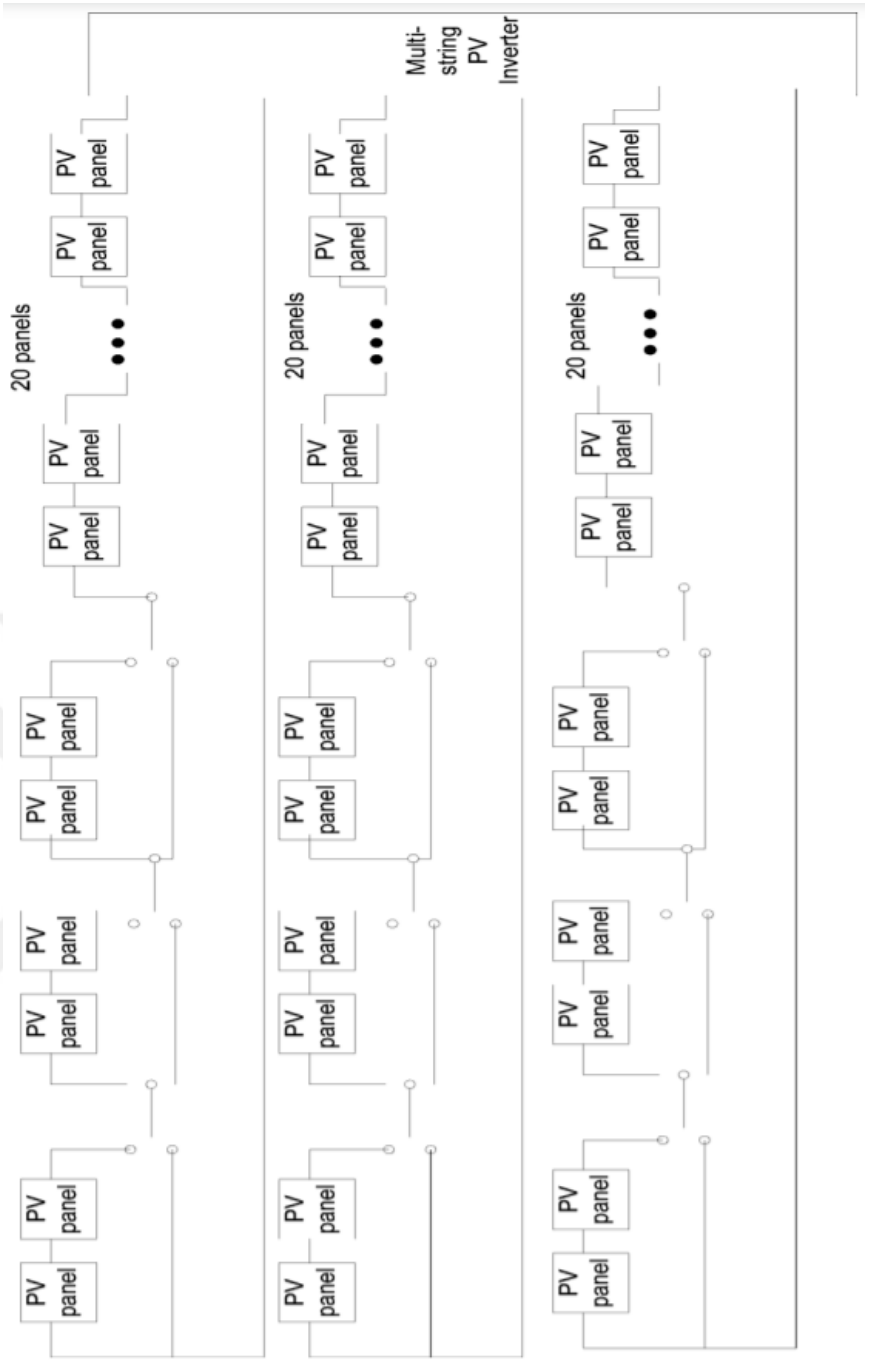

Figure 35. An Example of the Applied Control on a Typical PV Plant

VI. THE ISLANDING DETECTION METHOD EXPLAINED

A. Islanding Detection Methods and Their Types

Islanding is the condition when a segment of the utility framework that consist of both of load and generation is isolated from the rest of the utility system and yet stays energized. The confinement point is for the most part on the low voltage distribution line when an islanding condition exists, however islanding may likewise happen on the higher voltage conveyance or transmission lines when huge quantities of PV and other circulated generations are available.

The islanding condition is described as undesirable condition and there are many reasons to why it should be prevented with PV or any other distributed generation (e.g., safety, liability and maintaining the quality of the energy or power delivered to the end consumer).

The potential additional hazard that could be caused by the islanding mode to the utility line worker has been a center topic for the extensive discussions to why we needed anti-islanding PV inverters.

Various methods have been developed to detect an islanding mode occurrence in PV applications. These methods can be classified in three categories that are [32]:

- Passive IDM:

These methods basically monitor selected parameter (e.g., voltage and frequency and/or their characteristics) and make the inverter stop conversion of the power when these parameters deviate from the normal specified conditions.

- Active IDM:

These methods rely on monitoring the response of the connected circuit after introducing a disturbance to it to determine if the utility grid with its stable frequency, voltage and impedance is still connected.

- IDM not Resident in the Inverter and Generally at the Utility Level

The techniques that are not present in the inverter are commonly constrained by the utility or have interchanges between the inverter and the utility to influence an inverter shut down when needed.

Although they are mostly technology neutral, simple and easy to implement, Passive IDMs may fail to detect the islanding occurrence when the difference between the power generated by the DG and the one consumed by the load is small. The loading conditions under which islanding recognition would neglect to operate inside the specified time is considered as a Non-Detection Zone (NDZ). Conventional passive IDMs dependent on under/over voltage protection (UVP/OVP) will detect a bogus islanding condition during framework voltage deviations and subsequently don't comply to the new voltage ride-through (VRT) guidelines given in IEEE Std. 1547-2018. A portion of the advanced passive IDMs which recognize the islanding condition by looking at the wave, the harmonic substance, or the standardized logarithmic vitality entropy present in the voltage at the point of common coupling (VPCC) lessens or don't display NDZ. These strategies require execution of channels and process changes like Fast-Fourier or Wavelet Packet transform for identifying the islanding condition, which further builds the computational load and intricacy of the framework. In the event of active IDMs, the NDZ is insignificant or gets wiped out, yet, as previously explained, persistently infuses a limited quantity of controlled aggravation into the framework. The variety caused by the infused aggravation is monitored to recognize an islanding condition. A portion of the active methods are relevant just for three phase frameworks. The majority of the dynamic methods are commonly slow to identify, technology explicit, and incidental design of the control circuit may have negative effect on the utility grid. Also, there are different active IDMs which depend on the positive feedback impact. The feedback impact drives the framework to a temperamental state during the event of network disengagement. Be that as it may, the viability of these strategies relies on the estimation of the feedback gain. A higher estimation of feedback gain assists with identifying the islanding condition quick however confines the power transfer ability of the DG framework. Additionally, an exceptionally huge estimation of increase makes

the framework precarious significantly under network associated conditions and in this way triggers aggravation stumbling. hybrid IDMs joins active and passive techniques to separate the advantages of both and are more complex by consequence.

It is inappropriate and non-viable to incorporate computationally involved and complex IDM in the case of OCC based inverters. The active IDM presented in [6] is suitable for an OCC based inverter. In this technique, the islanding mode is detected by asymmetrically injecting subharmonic currents in two out of three phases which makes this IDM inappropriate for single-phased systems and injects subharmonics disturbances onto the grid. The IDM used in thesis is a simple passive method that relies on the feedback nature of the OCC based inverter. Soon after the disconnection of the utility grid, the built-in feedback nature of the system drives the Voltage at the Point of Common Coupling (VPCC) out of the operating limits triggering the UVP/OVP (Under/Over Voltage Protection) mechanism so that the inverter gets disconnected from the PCC.

B. Passive IDM Based on OCC Switching Scheme [33]

In this study, we are going to apply the IDM to the before mentioned microgrid system (figure 30), the IDM in study is based on an OCC based 3-phase inverter that is shown in figure 36 while its control is shown in figure 37. As commanded by the MPPT block in a closed loop, the DC link voltage Vdc is maintained equal to V_{ref}, and therefore keeping the real power of the system is regulated.

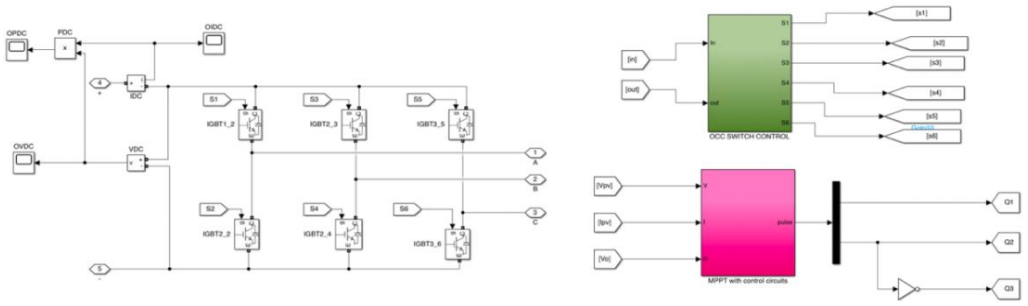

Figure 36. Three-Phase Grid-Connected PV Inverter System and Control Blocks (OCC Control Block and MPPT Block)

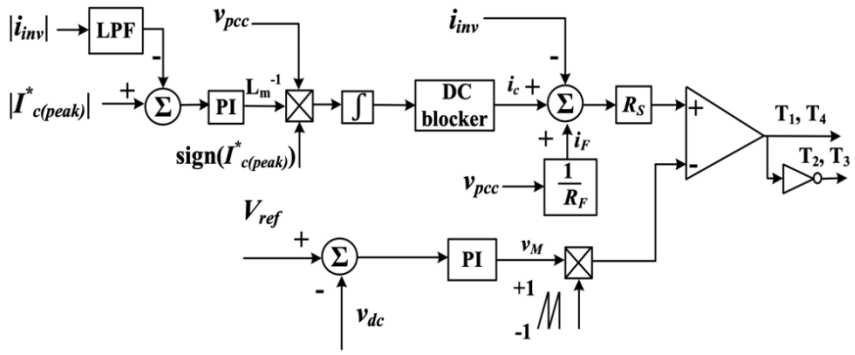

Figure 37. Block Diagram of the OCC Switching Scheme

The control signal V_M, that decides the magnitude of the carrier signal used for the PMW generation, is produced by the PI controller present in this feedback loop. Changing the emulated reactive current component i_c enables us to shift the reactive power of the framework. This is accomplished in shut circle by managing the size of the inverter current ($|i_{inv}|$) equivalent to the reference set ($|I^*_{c(peak)}|$). The normal estimation of inverter output voltage in one switching cycle is given as,

$$v_I = \frac{v_{dc} R_S}{v_M}\left(\frac{v_{pcc}}{R_F} + i_c - i_{inv}\right)$$

Equation 42

Where R_s represents the gain constant, R_F^{-1} represent the transconductance gain of the voltage sensor in the voltage feedback loop.

As we can deduct from the equation (42), the feedback nature of the OCC scheme gives the dependence of the inverter output voltage on the inverter current and the VPCC. This element drives the VPCC away from the ordinary working conditions during islanding so the UVP/OVP mechanism will detach the inverter from PCC. As prescribed in IEEE Std. 1547-2018, the maximum time to detect and islanding occurrence is 2 second (traditional passive IDM fails to detect the islanding within this range) and the allowable operating range of VPCC is 88-110% of the nominal voltage (regular inverters could stay connected of a wider range of 50-120%). The base ride-through time t_{rt} as a component of nominal voltage ordered in IEEE Std. 1547-2018 is appeared in Figure 38. The islanding can be identified if the feedback system drives the

VPCC past the ordinary working extent for period more prominent than t_{rt}. Under such conditions, the UVP/OVP instrument dactuated and the inverter is separated from PCC.

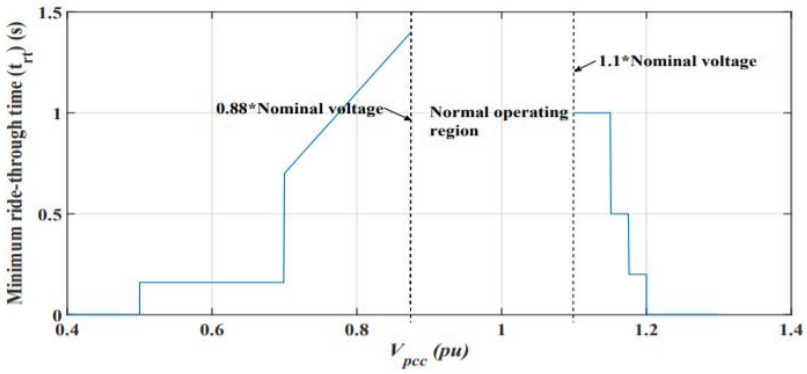

Figure 38. Minimum VRT Time as a Function of V_{pcc} (pu).

C. Feedback Response Model of The System

Figure 39 shows the linear equivalent circuit for the OCC based PV inverter framework with the test load during islanding mode. From the equation 3, the inverter in figure 5 is demonstrated in form of a three controlled voltage sources that are connected in series. Thus, the output voltage can be expressed as:

$$v_I(t) = k_1\left(\frac{1}{R_F}v_{pcc}(t) + \frac{1}{L_m}\int v_{pcc}(t)dt - i_{inv}(t)\right)$$

Equation 43

Where L_m^{-1} is the integrating gin constant,

$$k_1 = \frac{v_{dc}R_S}{v_M}, \text{ and } \frac{1}{L_m}\int v_{pcc}(t)dt = i_c \quad (44)$$

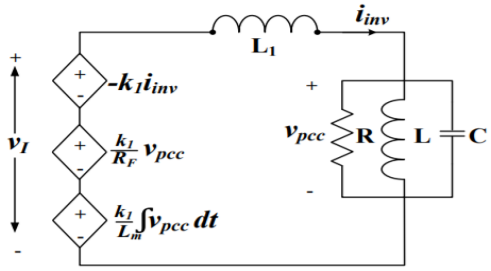

Figure 39. Equivalent Circuit Diagram for OCC Based System During Islanded Condition.

The block diagram of the system in Figure 39 above, is presented in figure 40 below and the articulation for $V_{pcc}(s)$ is given in equation (45) under it.

In equation, L_L (0), V_C (0) and I_{L1} (0) are the current flowing through the inductor L, the capacitor voltage C, and the current flowing through the inductor L_1 respective at the instant the gid disconnected.

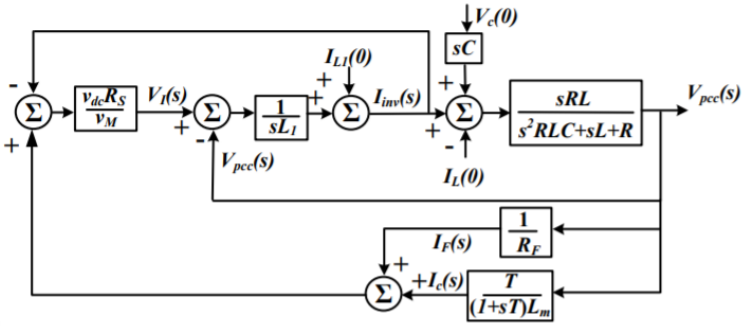

Figure 40. Block Diagram for OCC Based System During Islanded Condition.

$$V_{pcc}(s) = \frac{\begin{array}{c} L_m R_F \big(s^3 RLL_1 CV_C(0)T + s^2[RLL_1 T(I_{L1}(0) - I_L(0)) + RLCV_c(0)(L_1 + k_1 T)] \\ + s[RLL_1 I_{L1}(0) + RLCV_c(0)k_1 - I_L(0)RL(L_1 + k_1 T)] - I_L(0)RLk_1\big) \end{array}}{\begin{array}{c} s^4 RR_F LL_1 L_m CT + s^3 R_F L_m L(L_1 T - RC(L_1 + k_1 T)) + s^2 L_m[R_F L(L_1 + k_1 T) + LRT(-k_1 + R_F) \\ + L_1 RR_F T + RR_F LCk_1] - sR_F[RL_m(L_1 + k_1 T) + L_m Lk_1 + L_m LR(-k_1 T + L_m)] + RR_F L_m k_1 \end{array}}$$

Equation 45

Expecting that the size of V_M and Lm created by the PI regulators given in Figure 37 stays steady during the occasion, time space articulation for $v_{pcc}(t)$ is resolved from 39 [33] as:

$$v_{pcc}(t) = Ae^{-\frac{t}{\tau_A}} + Be^{-\frac{t}{\tau_B}} + De^{-\frac{t}{\tau_C}} cos(\omega_d t + \phi),$$

Equation 46

Where A, B, and D are voltage constants whose worth is reliant upon the framework boundaries and starting states of inductor flows and capacitor voltages. While the third term is a sinusoidally modulated exponentially varying voltage of the constant τ_c and frequency y ω_d, the first and second term are to represent the exponentially decaying voltages with time constants τ_a and τ_b respectively. Usually, the first and second terms in (46) are fast decaying and negligibly small compared to the third term. In this case, the VPCC can approximate with the third term and its RMS value can be approximately expressed as:

$$V_{pcc}(t) \approx V_{pcc}(0)e^{-\frac{t}{\tau_C}}$$

Equation 47

Where V_{pcc} (0) is the RMS value of the voltage at the moment when the grid disconnects, and the time constant τ_C chooses the rate at which the RMS estimation of VPCC rots or rises. Depending on the operating condition, the numeric value of τ_C is a 4th order function of the various parameters given in figure 39. If τ_C is large, the VPCC takes longer time to stray away from standard operation conditions which makes the islanding mode detection more difficult. The value of τ_c assume positive or negative values based on the sing of ΔP at the time of disconnection of the grid. When ΔP < 0, the system is considered unstable with a negative τ_c and the VPCC's Rms value rises exponentially. As opposed to when ΔP < 0, the τ_c is positive in a stable system where the RMS value of the VPCC decays. The time constant τ_c becomes larger as ΔP approaches 0, and in this case the IDM may fail to detect the islanding condition within the set forth time.

Figure 41 shows the typical nature of the bode plot for positive and negative value of of ΔP (ΔP = 0.01 pu, ΔP = −0.04 pu and Qf = 2.5). We can see that the system is stable when or ΔP>0 and the VPCC exponential decay effect caused by the negative feedback is shown in figure 42. At the same time, the magnitude plot for ΔP<0 is given in Figure 42. As it can be seen, it is below the 0 dB line, the phase margin of the system is infinity and the system is unstable. The VPCC shows an exponential increase as a response to the positive feedback which can be clearly seen in figure 42.

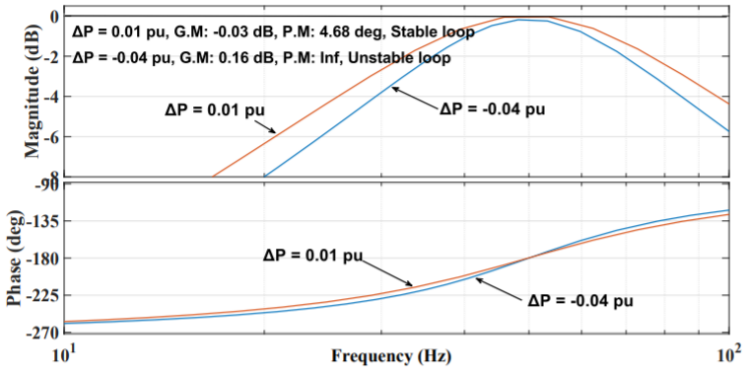

Figure 41. Bode Plot of the System After Grid Disconnection

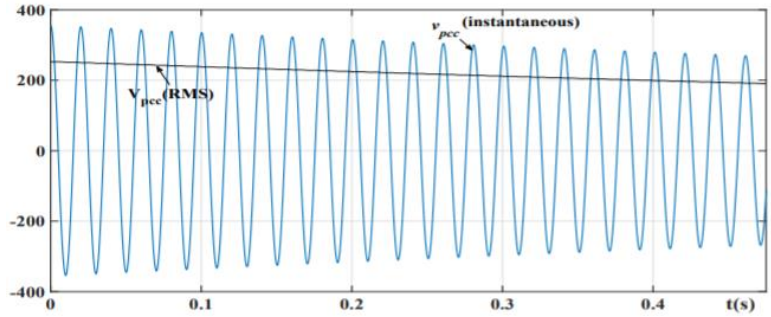

Figure 42. Response of the System After Grid Disconnection for ΔP = 0.01 pu

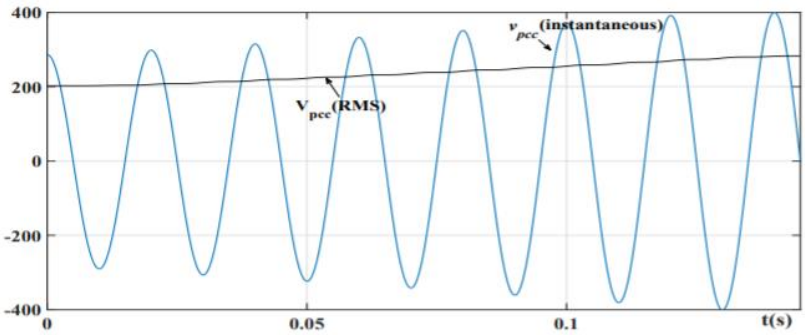

Figure 43. Response of the System After Grid Disconnection for ΔP = −0.04 pu

D. Design Consideration

In case of a grid detachment, the feedback system drives the VPCC past the ordinary working range. The UVP/OVP disengage the inverter from the PCC subject to the limitations forced by the V_{RT} guidelines regarding t_{rt} given in Figure 39. The islanding can be detected within 2 s only if the voltage has attained certain values with in a time limit (t_{lim}) given as.

$$t_{lim} = 2 - t_{rt}$$

Equation 48

The estimations of t_{rt} and the comparing t_{lim} as an element of V_{PCC} is given in Table I. The islanding can be distinguished if any of the t_{lim} given in Table 1 is fulfilled by the framework and the condition for acceptable assurance of islanding condition is given by $-11.2s < \tau_C < 5.15s$. By considering the voltage limit and the t_{lim}, the value of τ_c is calculated from (47) as given in table 1 above. If $\tau_c > 5.15$ and $\tau_c < -112$, none of the t_{lim} given in table 1 below get satisfied and eventually results in NDZ.

Table 1. Ride-Through Time and Time Limit for Different Vpcc (PU)

S1. No	V_{pcc} (pu)	t_{rt} (s)	t_{lim} (s)	TC (s)
1	1.2^{+}	0	2	-11.0
2	1.175^{+}	0.2	1.8	-11.2
3	1.15^{+}	0.5	1.5	-10.7
4	1.1^{+}	1	1	-10.5
5	0.88^{-}	1.42	0.58	4.54
6	0.7^{-}	0.16	1.84	5.15
7	0.5^{-}	0	2	2.88

As it has been explained in the previous section, the mathematical estimation of $\boldsymbol{\tau}_c$ relies upon the boundaries of the fourth order framework based on consideration and working conditions such as ΔP. A large portion of the boundaries of the framework like R, L, C, L_1, k_1, and L_m are fixed by different contemplations or working conditions and RF is the only parameter which can be changed for altering the estimation of $\boldsymbol{\tau}_C$. Figure 43 shows a plot of $\Delta P(\%)$ v/s R_F for the giving limiting values of $\boldsymbol{\tau}_C$, where the nominal power of the inverter is of the same value as the load connected and $Q_f = 2.5$. The IDM will not be able to identify an islanding condition within the specified time if ΔP lies between the two curves. It can be observed that the NDZ reduces as R_F increases. However, according to stability condition that is mentioned in [35] and [36], the value of R_F cannot be increased beyond a certain limit. This condition for stable operation of the converter is given as follows:

$$\frac{1}{R_F} > \frac{T_S}{2L_1 v_{dc}} v_{pcc(peak)} + \frac{P_{inv}}{{V_{pcc}}^2}$$

Equation 49

Where T_S is the switching period. Figure 44 shows as well the stable operating region of the converter where the optimum value of R_F can be chosen such that the system is stable and the NDZ is as minimal as they could be.

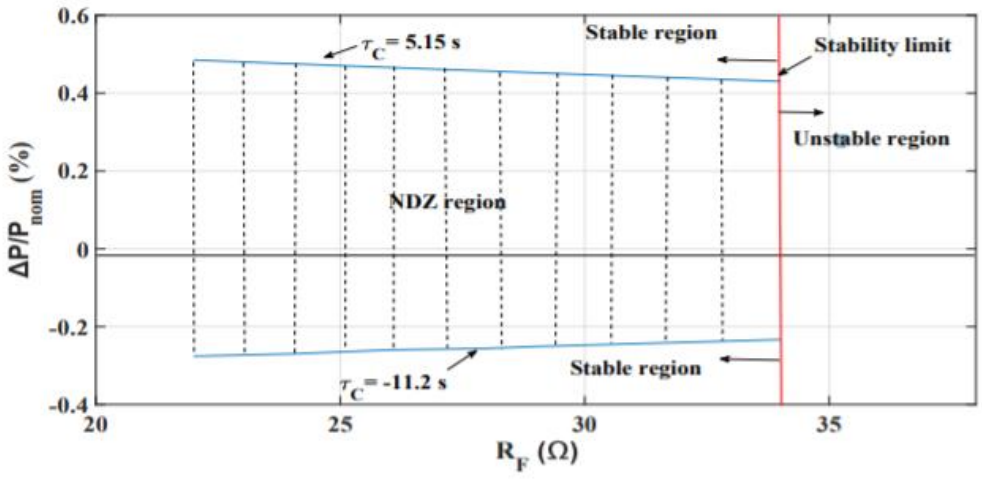

Figure 44. $\Delta P/P_{nom}$ (%) v/s R_F for the Given Limiting Values of τ_C

The traditional passive IDMs based on voltage and frequency limits have a larger NDZ compared to the IDM used for this study, the NDZ for these methods is given in [34] as:

$$-17.36\% \leq \frac{\Delta P}{P_{nom}} \leq 29.13\%$$

Equation 50

$$-7.15\% \leq \frac{\Delta Q}{P_{nom}} \leq 4.92\%$$

Equation 51

Where P_{nom} is the inverter's nominal power. The NDZ for the IDM used in this study is determined for the optimum value of R_F =30 Ω and given in figure 45 below. As it can be seen, the voltage is based IDM is very successful at detecting islanding condition. The NDZ for this IDM is less than 1.5% of the NDZ exhibited by traditional IDM given in (52) and is given as:

$$-0.25\% \leq \frac{\Delta P}{P_{nom}} \leq 0.45\%$$

Equation 52

Since it relies on the mismatch of the reactive power, the frequency-based IDM is not a suitable method to be adapted because it has bigger NDZ which has limit almost equals to that of traditional passive IDM. On the other side, frequency deviation-based IDM is a good to be incorporated into the system along with the voltage deviation voltage-based IDM used in this study without any extra load.

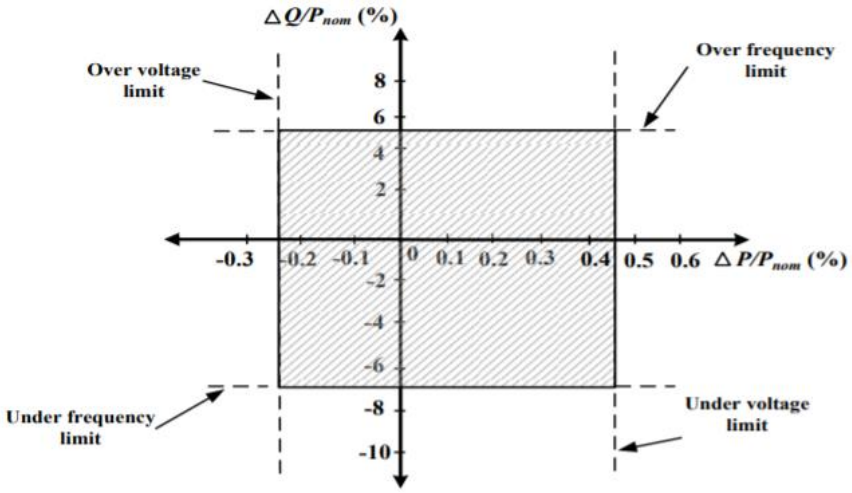

Figure 45. NDZ for the IDM used in the Study

VII. IMPLEMENTATION, SIMULATION AND RESULTS

The discussed IDM for the OCC based grid tied three phase inverter system that is given in figure 36 is simulated using MATLAB/Simulink. The inverter is installed in the microgrid in the Smart distribution gird topology that incorporated, TEIWM microgrid. The system under consideration and its simulation is shown in figure 46 as a whole.

The control unit is shown in figure 47 and in it we can see the MPPT control circuits as well as the Unfolding and switch control (OCC).

The parameters chosen for the simulation studies are shown in table II. The steady state results of the grid tied three-phase inverter (the grid voltage (Vg), VPCC (Vpcc), grid current (i_g), inverter current (i_{inv}) and inverter Voltage (V_{inv})) are shown in figure 56. The test load is chosen with the end goal that the power produced by the source is devoured by the load and the current took care of to the grid is unimportant.

Table 2. Simulation Parameters

Parameters	Values
Grid	230 V, 50 Hz
Inverter	1kW
Series inductor	10 mH
Dc-link capacitor	3000 μF
R_F	30 Ω
K_p and K_I	0.01 and 9 s^{-1}

In order to test this IDM, the grid breaker in figure 46 is opened in order to create an islanding mode. With $\Delta P = 0$ and $\Delta Q = 0$, both reactive and real powers of the load and the inverter are maintained at standard test condition. The reactive load is adjusted so the resonant frequency of the islanded circuit is

as near the ostensible frequency as could reasonably be expected, which brings about zero reactive power under testing conditions [36].

A. Quality Factor's Effect

The impact of progress in the quality factor of the load has been researched and a greatest quality factor of 2.5 is considered for the islanding recognition test. For the given inverter under test, the load associated is equivalent to the ostensible inverter power and the reactive power is balanced at 100% adjusted condition ($\Delta Q = 0$). In order to test inverter at hand, the grid is disconnected at the mark of 3s. figure 53 shows the value of VPCC during both the grid-connected and islanding phases as well as the UVP/UVP trigger signal. As we can see, the OVP is acting simply after the VRT prerequisites are fulfilled at VPCC more prominent than 1.2 pu, when the comparing estimation of t_{rt} is equivalent to 0s.

The islanding condition detection period increase as quality factor increases, and the expanded proportion of energy put away in the LC tank in correlation with the rate at which vitality is disseminated in the resistive burden will in general support the motions in VPCC for a more extended span of time and henceforth makes islanding recognition troublesome.

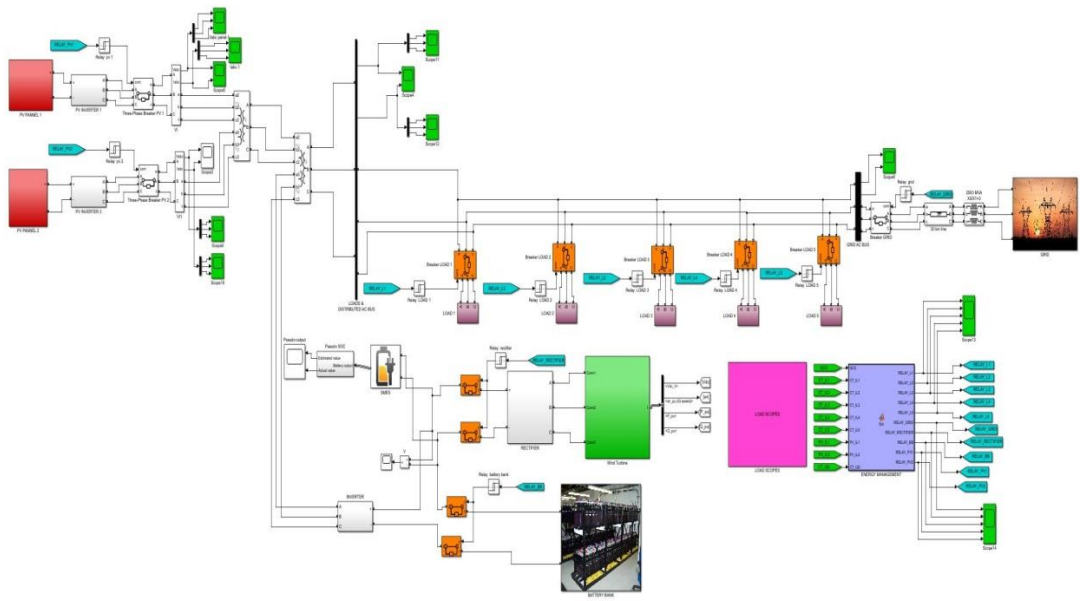

Figure 46. The System in Study

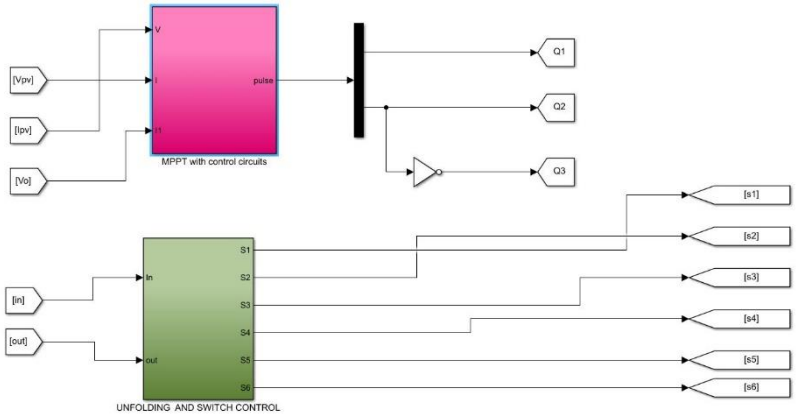

(a)

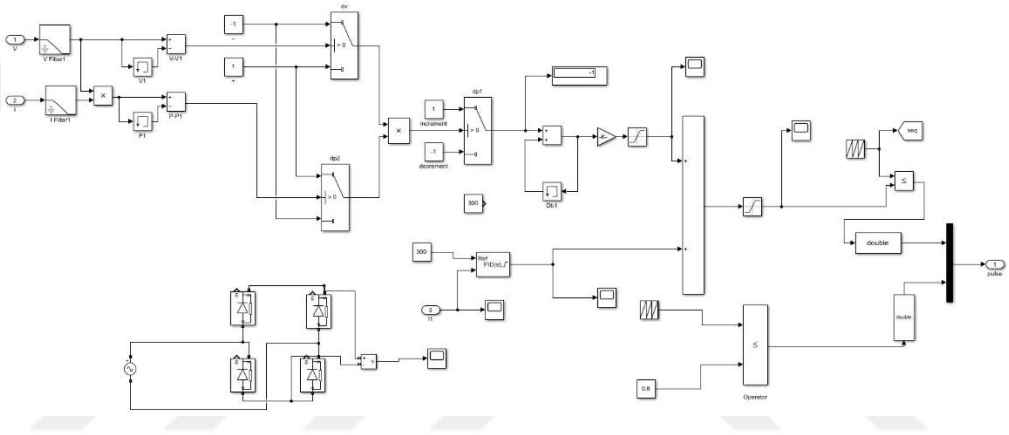

(b)

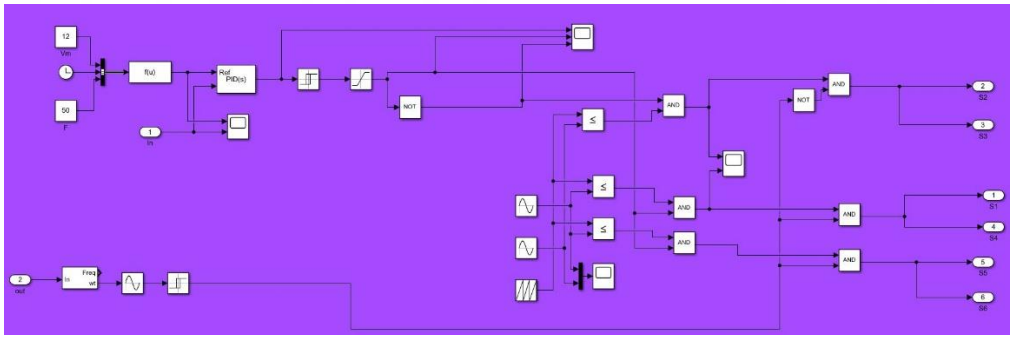

(c)

Figure 47. (a) MPPT and Switch Control Command Blocks (b) MPPT Circuit (c) unfolding and switch control (OCC)

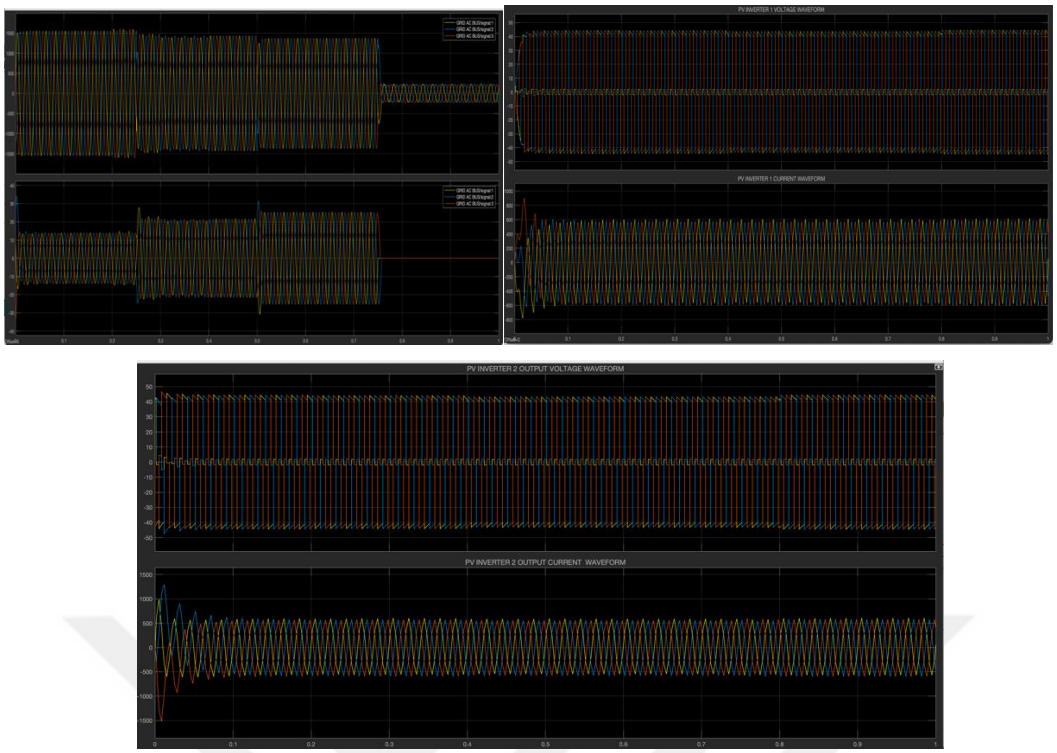

Figure 48. The Grid Voltage (*V*g), Grid Current (i_g),1st PV Inverter Current and Voltage Waveforms (additional) 2nd PV inverter Current and Voltage waveform

By implementing the micro grid topology and the energy storage management in [24] and incorporating the OCC inverter (with the discussed IDM) as shown in figure 48 above we have been able to obtain the results shown below.

As it can be seen from figure 49 of the PV and IV characteristic graph, the MPPT power drawing control is functioning as it should and the 3-phase voltage as well as the current produced by the PV panels as shown in figure 48 (2nd and 3rd pictures). We can see that the DC current/voltage drawn from the PV panels is successfully converted into a stable AC current/voltage

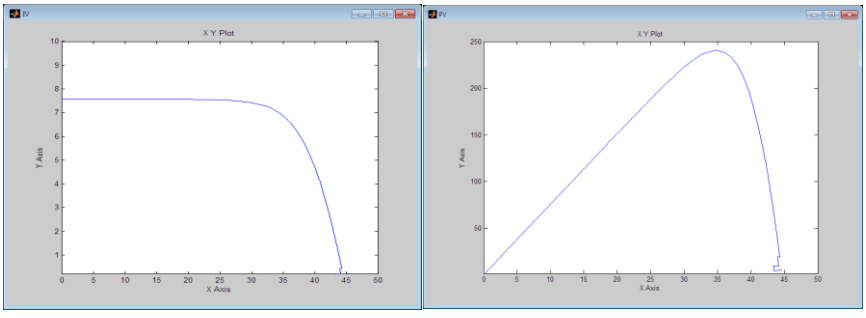

Figure 49. IV and PV Characteristics

As defined in section 50, the pseudo SoC that is assigned to the batteries in order to avoid to any unnecessary load rejections is implemented and can be verified in figure 51 below.

Figure 50 shows both the estimated and actual SoC. It can be seen that the estimated Soc is lower than the actual SoC, which is why a new set of SoC has been associated to encounter the deficit and the gap between the actual SoC and the estimated SoC.

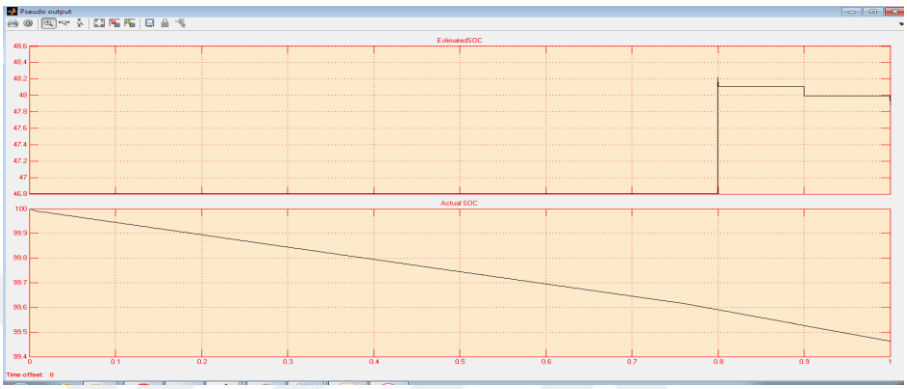

Figure 50. Battery Pseudo Output Concept (SoC vs Estimated SoC)

Figure 53 is a plot of the Loads and distributed AC bus, current and voltage. As it can be seen, the voltage and current signal change according to the loads demand which means that the power generation system is able to satisfy the demand of the loads. With the energy management strategy in place, we can focus more about the islanding condition and how the implemented IDM is working in a 3-phase environment as opposed to single-phase environment as well as how does it compare to other IDMs.

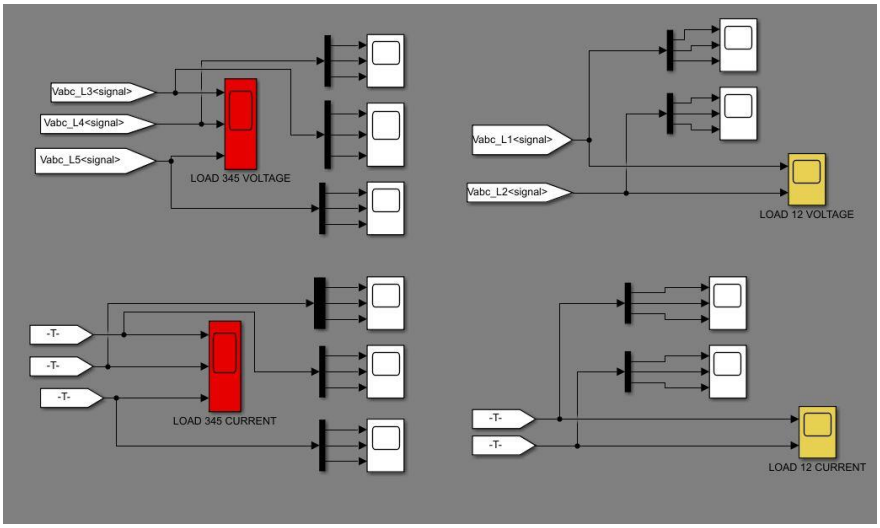

Figure 51. Plotting the Loads 1, 2, 3, 4 and 5

The following plots are taking from the highlighted scopes in figure 56. These plots show that the load and energy storage management is a successful and by protecting the system from the islanding mode by early detection and shutting down the isolated section, the system energy consumption is smoother and more efficient.

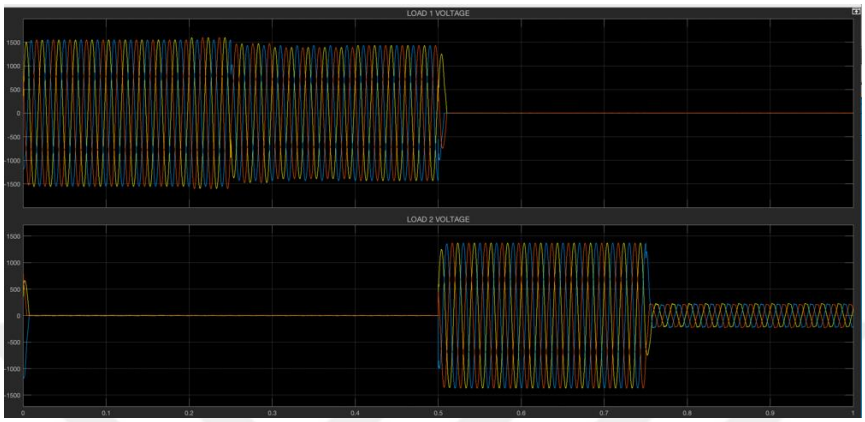

Figure 52. Voltage of Loads 1 and 2

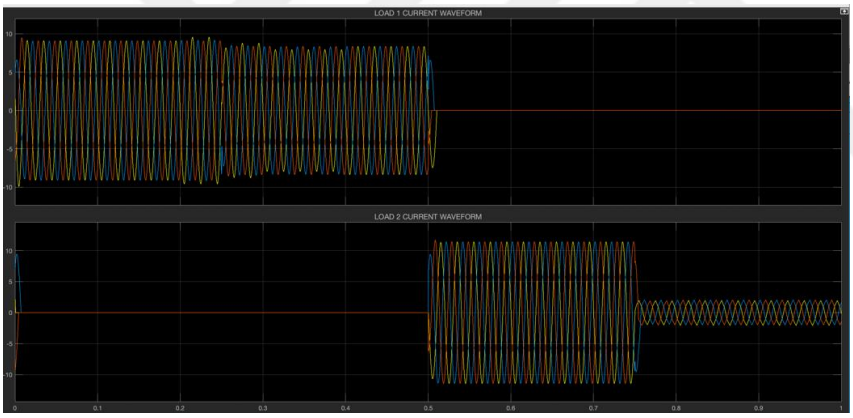

Figure 53. Current of Loads 1 and 2

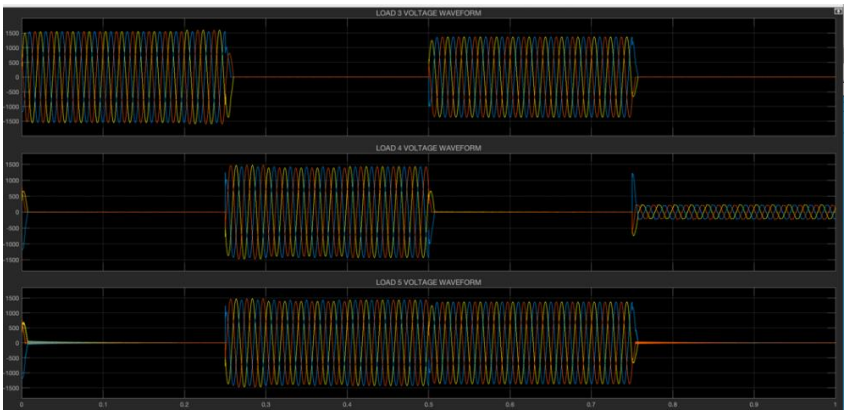

Figure 54. Voltage of Loads 3, 4, and 5

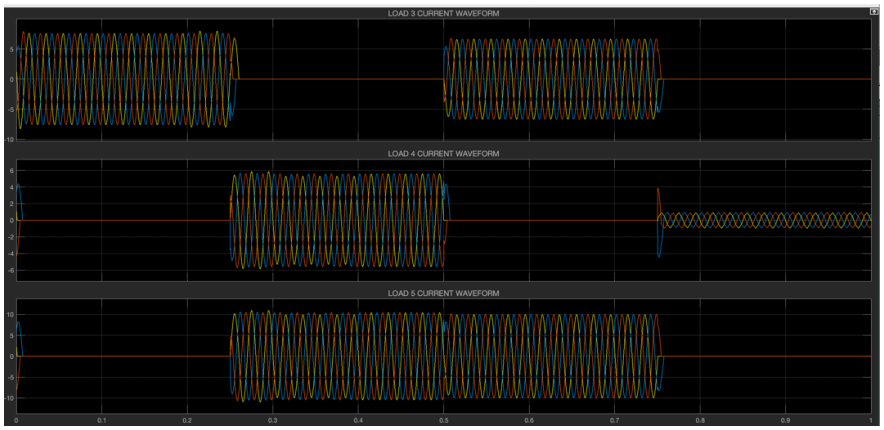

Figure 55. Current of Loads 3, 4, and 5

From the figures 48 (1st picture), 52, 53, 54, 55, it takes about 52 seconds to detect the islanding condition and to shut down the power on the whole system.

For a single-phase inverter at high capacity where quality factor is 2.5, inverter active power 0.8 pu, inverter reactive power -0.6 pu, load active power 0.8 pu, and load reactive power -0.6 pu, this IDM is capable of detecting an islanding condition in 0.76 seconds [33]. This mean that the simulation is a success and we were able to achieve the results that we expected. The great advantage that this method grants us is that NDZ is significantly smaller than other traditional passive methods given in [34] provide (less than 1.5%).

More extensive testing conditions as well as experimental studies are to be found in the [25] while experimental results of the microgrid topology and energy management is presented in [24].

VIII. CONCLUSION

In this thesis research, we explored this novel passive IDM that relies on the inbuilt feedback nature of the OCC scheme that drives the VPCC out of the operating region during an islanding occurrence and the feedback response model is developed in order to study the variation in VPCC during islanding mode. This IDM was initially designed of single-phase inverters, but in this thesis, it was tested on three-phase inverter. Under the new standard requirements with negligible NDZ, the efficiently working IDM does not require additional software or disturbance injection for its implementation. This IDM is not generic and only works for OCC based inverters. Which we have implemented in a microgrid-based smart grid topology. In this thesis, the said topology had an improved energy storage management and PV active power control applied to it. In order to improve the energy storage management, the pseudo-SoC concept has introduced. Additionally, a PV-plant control strategy that is based on remote control of the PV strings actuators is described and applied. The mentioned strategy is by no mean invasive to the inverter. The strategy considers the past SoC of batteries and consolidates appropriately the SoC determination with estimations by RES and stacks and focused on control activities. Which is why it have a control infrastructure and iterative algorithms that are implemented into the microgrid facilities and can be applied to all RES included. The activity of the microgrid with the improved control framework and the iterative algorithm is compared, regarding dependability, to a microgrid with an alternate control methodology and topology.

IX. REFERENCES

BOOKS

BOWER, W., & ROPP, M. E. (2002). '**Evaluation of islanding detection methods for photovoltaic systems on distribution protection**'. Report IEA PVPS T5-09: 2002. [32]

PERLIN, J. (2013). **'Let it Shine: The 6,000-year Story of Solar Energy'**. San Francisco (USA): New World Library, 2013. [2]

WOLFE, P. R. (2018). '**The Solar Generation: Childhood and Adolescence of Terrestrial Photovoltaics'** IEEE Press, New Jersey.

WOLFE, P. R. (2018). **The Solar Generation: Childhood and Adolescence of Terrestrial Photovoltaics**, First Edition.

ARTICLES

ACHAIBOU, N., HADDADI, M., & MALEK, A. (2012). Modeling of Lead Acid Batteries, in **PV Systems**. [38]

BLAABJERG, F., CHEN, Z., & KJAER, S. B. (2004). "Power electronics as efficient interface in dispersed power generation systems", **IEEE Transactions on Power Electronics,** vol. 19, no. 5, pp. 1184-1194, 2004. [10]

BOUTALIS, Y., KOTTAS, T., & CHRISTODOULOU, M., (2009). "Adaptive estimation of fuzzy cognitive maps with proven stability and parameter conver- gence", **IEEE Trans. Fuzzy Syst.**, vol. 17, no. 4, pp. 874–889, Apr. 2009. [23]

BRANCO, C. G. C., TORRICO-BASCOPE, R. P., CRUZ, C. M. T., & DE A LIMA, F. K. (2013). "Proposal of three-phase high-frequency transformer isolation UPS topologies for distributed generation applications," **IEEE Trans. Ind. Electron.,** vol. 60, no. 4, pp. 1520-1531, Apr. 2013. [28]

CHATTERJEE, K., GHODKE, D. V., CHANDRA, A., & AL-HADDAD, K. (2009). "Simple controller for STATCOM-based var generators," in **IET Power Electron.,** vol. 2, no. 2, pp. 192-202, March 2009. [37]

CHEN, W., SHEN, H., SHU, B., QIN, H., & DENG, T. (2007). Evaluation of performance of MPPT devices in PV systems with storage batteries. **Renewable Energy,** Volume 32.

CHEN, Y., & KEYUE MA SMEDLEY. (2008). One-Cycle-Controlled Three-Phase Grid-Connected Inverters and Their Parallel Operation. **IEEE Transactions on Industry Applications,** Vol. 44, No. 2, March/April 2008. [13]

DE BRABANDERE, K., VANTHOURNOUT, K., DRIESEN, J., DECONINCK, G., & BELMANS, R. (2007). "Control of microgrids" in **Proc. IEEE Power Eng. Soc. General Meeting,** Tampa, FL, USA, 24-28 June 2007. [24]

EHRET, C.H., PILLER, S., SCHROER, W., & JOSSEN, A. (2000). "State-of-charge determination for lead-acid batteries in PV-aplications" in **Proc. 16th Eur. Photovoltaic Solar Energy Conf.**, Glasgow, U.K., 2000.

GHODKE, D. V., CHATTERJEE, K., & FERNANDES, B. G. (2008). "Modified one-cycle controlled bidirectional high-power-factor AC-to-DC converter", in **IEEE Trans. Ind. Electron.,** vol. 55, no. 6, pp. 2459-2472, 2008. [35]

IEEE Standard Conformance Test Procedures for Equipment Interconnecting Distributed Resources with Electric Power Systems, **IEEE Std 1547.1**, 2005. [36]

JAGANMOHAN REDDY, Y., PAVAN KUMAR, Y. V., SUNIL KUMAR, V., & PADMA RAJU, K. (2012). "Distributed ANNs in a layered architecture for energy management and maintenance scheduling of renewable energy HPS microgrids", in **Proc. IEEE Int. Conf. Adv. Power Conversion and Energy Technol.**, 2012, pp. 1-8. [29]

KEYUE, M., SMEDLEY, SLOBODAN ĆUK, (1995). "One-Cycle Control of Switching Converters", **Transactions on Power Electronics**, VOL. 10 NO.6, November 1995. [12]

KIANMANESH, A. M., & AKHAVAN, A. (2020). Power Control of Grid-Connected Inverters Using One-Cycle Control Method for PV Systems. **2020 Zooming Innovation in Consumer Technologies Conference (ZINC).** 26-27 May 2020, Novi Sad, Serbia. [16]

KRAY, D. & SAUER, D. U. (1998). "Neuro-methoden zur prognose und fehlererkennung durch analyse vor daten aus monitoring-systemen", **Internationales Sonnenforum**. Koln, 1998.

MALLWITZ, R., & ENGEL, B., (2010). 'Solar power Inverters'. **CIPS 2010**, March, 16-18, 2010, Nuremberg/Germany. [8]

MEINHARD, M., CRAMER, G., ENGEL, B., & VICTOR, M., (2007). New Generation of PV Inverters with Advanced Power Electronics Packaging Concept for Highest Reliability and Minimum Assembly Time in Mass Production. **22nd European PV Solar Energy Conference**, Milan, 2007. [7]

MINGUYU, W., YAQIAN, H., & CHENGYU, X. (2005). One-Cycle Control Based Voltage Source Inverters. **2005 International Conference on Electrical Machines and Systems,** 27-29 Sept. 2005. Nanjing, China. [15]

MOLINA, M. G. (2012). "Distributed energy storage systems for applications in future smart grids," in **Proc. 6th IEEE PES Transm. Distrib.: Latin America Conf. Expo.,** Montevideo, Uruguay, 3-5 Sept. 2012, pp. 1–6. [31]

PASCOE, E., & ANBUKY, A. H. (1999). "Estimation of VRLA battery capacityusing the analysis of coup de fouet region", **INTELEC,** Copenhagen, Denmark, 9-9 June 1999.

PILLER, S., PERRIN, M., & JOSSEN, A. (2001). "Methods for state-of-charge determination and their applications", **J. Power Sources,** vol. 96, pp. 113–120, 2001. [26]

QIAO, C., & SMEDLEY, K. M. (2001). "One-Cycle-Controlled Three-Phase Grid-Connected Inverters and Their Parallel Operation" in **Conf. Rec. IEEE IAS Annu. Meeting,** Chicago, IL, Sep./Oct. 2001, vol. 4, pp. 2675–2682. [14]

REDDY, V. R., & E S, S. (2019). A Feedback based Passive Islanding Detection Technique for One Cycle Controlled Single Phase Inverter used in Photovoltaic Systems. **IEEE Transactions on Industrial Electronics,** 1–1. Volume: 67, pp 6541 – 6549, 05 September 2019. [33]

REKIOUA, D. & MATAGNE, E. (2012). "Power electronics modeling," in **Optimization of Photovoltaic Power Systems Modelization, Simulation and Control,** Springer, Verlag, London, 2012, pp. 89-112. [9]

SANTACANA, E., RACKLIFFE, G., TANG, L., & FENG, X. (2010). "Getting smart-with a clearer vision of the intelligent grid, control emerges from chaos", **IEEE Power & Energy Mag.,** vol. 8, no. 2, pp. 41–48, 2010. [22]

SRIDHAR, R., JEEVANANATHAN, DR., THAMIZH SELVAN, N., & SAIKAT BANERJEE (2010). Modeling of PV Array and Performance Enhancement by MPPT Algorithm. **International Journal of Computer Applications**, Volume 7, 2010. [4]

STIMONIARIS, D., TSIAMITROS, D., & DIALYNAS, E. (2016). Improved Energy Storage Management and PV-Active Power Control Infrastructure and Strategies for Microgrids. **IEEE Transactions on Power Systems,** 31(1), 813–820. doi-10.1109/tpwrs.2015.2389954. [17]

STIMONIARIS, D., TSIAMITROS, D., KOTTAS, T., ASIMOPOULOS, N., & DIALYNAS, E. (2011). "Smart grid simulation using small-scale pilot installations-experimental investigation of a centrally-controlled microgrid," in **Proc. IEEE PowerTech,** Trondheim, Norway, 19-23 June 2011. [21]

STIMONIARIS, D., TSIAMITROS, D., POULAKIS, N., KOTTAS, T. & DIALYNAS, E. (2014). "Experimental-based improvements of the flexibility of RES and energy storage plants," presented at **the MedPower 2014 Conf.,** Nov. 2–5, 2014. [18]

STIMONIARIS, D., TSIAMITROS, D., POULAKIS, N., KOTTAS, T., KIKIS, V. & DIALYNAS, E. (2011). "Investigation of smart grid topologies using pilot installations-experimental results," in **Proc. IEEE ISGT**, Manchester, UK, 5-7 Dec. 2011. [20]

SUNEEL RAJU PENDEM, S. MIKKILI. (2018). Modeling, simulation, and performance analysis of PV array configurations (Series, Series-Parallel, Bridge-Linked, and Honey-Comb) to harvest maximum power under various, **Partial Shading Conditions**, pp. 795-812, 25 Sep (2018).[3]

TSENGENES, G. & ADAMIDIS, G. (2011). "A multi-function grid connected PV system with three-level NPC inverter and voltage-oriented control". **Solar Energy,** vol. 85, pp. 2595–2610, 2011.

TSIAMITROS, D., STIMONIARIS, D., POULAKIS, N., ZEHIR, M. A., BATMAN, A., BAGRIYANIK, M., OZDEMIR, A., & DIALYNAS, E. (2014). "Advanced energy storage and demand-side management in smart grids using buildings energy efficiency technologies" presented at **the IEEE Innovative Smart Grid Technologies 2014 Conf.**, Istanbul, Turkey, Oct. 12–15, 2014. [19]

VANDOORN, T. L., RENDERS, B., DEGROOTE, L., MEERSMAN, B., & VAN-DEVELDE, L. (2011). "Active load control in Islanded microgrids based on the grid voltage", **IEEE Trans. Smart Grid,** vol. 2, no. 1, pp. 139–151, 2011. [25]

VECHIU, I., ETXEBERRIA, A., CAMBLONG, H., & VINASSA, J. M. (2011). "Three-level neutral point clamped inverter interface for flow battery/supercapacitor energy storage system used for microgrids," in **Proc. IEEE ISGT,** Manchester, U.K., 2011, pp. 1–6. [30]

YILDIRAN, N. (2016). Detailed Modeling of Solar Inverter. **Proceedings of the 2nd World Congress on Electrical Engineering and Computer Systems and Science (EECSS'16).** Paper No. EEE 141, Budapest, Hungary, August 16 – 17, 2016. [11]

ZHIHONG, Y.E., KOLWALKAR, A., ZHANG, Y.U., PENGWEI, D.U., & REIGH WALLING, (2004). "Evaluation of anti-islanding schemes based on nondetection zone concept", in **IEEE Trans. Power Electron.,** vol. 19, no. 5, pp. 1171-1176, Sept. 2004. [34]

DISSERTATION

HONES, H. P. (1994). "Elektrochemische energiespeicher in photovoltaischen anlagen", (Ph.D. dissertation), Renewable Energy Dept., Universitat Stuttgart, Stuttgart, Germany, 1994.

ELECTRONIC SOURCES

"**Sunny Island Installation Guide**," ver. 4,0 [Online]. Available: http://www.sma.de [27]

Energy conversion: Development of Solar Cells. (1998). Britannica. online, https://www.britannica.com/technology/solar-cell; October 21, 1998. [1]

Grid-Tied, Off-Grid, and Hybrid Solar Systems, Solar Reviews, (2019). July 2019 https://www.solarreviews.com/blog/grid-tied-off-grid-and-hybrid-solar-systems. [6]

How PV Cells Work. (2014). ucf.edu, 2014, www.fsec.ucf.edu/en/consumer/solar_electricity/basics/how_pv_cells_work.htm. [5]

APPENDICES

Appendix 1. Ethics Committee Decision

Appendix 1. Ethics Committee Decision

Appendix 1. Ethics Committee Decision

T.C.
İSTANBUL AYDIN ÜNİVERSİTESİ
LİSANSÜSTÜ EĞİTİM ENSTİTÜ MÜDÜRLÜĞÜ

YÜKSEK LİSANS TEZ DEĞERLENDİRME FORMU

Adayın		**Tez Danışmanı**
Adı Soyadı	MOHAMMED YASSINE EL HASSNI	Prof. Dr. Murtaza FARSADİ
Numarası	Y1813.300011	
Anabilim Dalı	Elektrik Elektronik Mühendisliği	
Bilim Dalı	Elektrik Elektronik Mühendisliği İngilizce	
Tez Konusu	Passive Islanding Detection Technique for Three-Phase Grid-Connected PV Inverter System	

Tez jüri üyeleri

Prof. Dr. Murtaza FARSADİ
Dr. Öğr. Üyesi Eylem Gülce ÇOKER
Prof. Dr. Ayşen DEMİRÖREN
Dr. Öğr. Üyesi Necip Gökhan KASAPOĞLU
Prof. Dr. Aydoğan ÖZDEMİR

Tezde kullanılan yöntem (birkaçının birden işaretleyebilirsiniz)

☐ Kuramsal ■ Sayısal ☐ Deneysel ☐ Diğer:.....

Tez içeriği, Proje konusu ile uyuşuyor mu ? ■ Evet ☐ Hayır

	Çok iyi	**İyi**	**Orta**	**Kötü**	**Çok kötü**
1.Tezde kullanılan yöntem uygun mu?	■	☐	☐	☐	☐
2.Tez özgün mü?	■	☐	☐	☐	☐
3.Tezdeki literatür taraması yeterli mi?	■	☐	☐	☐	☐
4.Tezde kullanılan yöntemin güncelliği nasıl?	■	☐	☐	☐	☐
5.Şekiller ve tablolar tezdeki bulguları yansıtıyor mu ?	■	☐	☐	☐	☐
6.Tezde sunulan bulgular yeterince tartışılmış mı?	■	☐	☐	☐	☐
7.Tezdeki bulgular, sonuçlar bölümünde iyi özetlenmiş mi?	■	☐	☐	☐	☐

Tez hakkında verdiğiniz kararın gerekçelerini yazınız. (Gerekirse ek sayfa kullanınız.)

BAŞARILI

Tez kabulu konusundaki görüşünüz

■ Değişikliğe gerek yoktur ☐ Şekil yönünden bazı değişiklikleri yapılması gerekir
☐ Reddedilmesi gerekir ☐ İçerik yönünden değişikliklere gerek vardır/yoktur

Öğretim Üyesinin		
Adı Soyadı,Ünvanı	**Prof. Dr. Murtaza FARSADİ**	
E-Posta		Tarih : 08.09.2021
Faks	:	
Telefon	:	İmza :

T.C.
İSTANBUL AYDIN ÜNİVERSİTESİ
LİSANSÜSTÜ EĞİTİM ENSTİTÜ MÜDÜRLÜĞÜ

YÜKSEK LİSANS TEZ DEĞERLENDİRME FORMU

Adayın		**Tez Danışmanı**
Adı Soyadı	MOHAMMED YASSINE EL HASSNI	Prof. Dr. Murtaza FARSADİ
Numarası	Y1813.300011	
Anabilim Dalı	Elektrik Elektronik Mühendisliği	
Bilim Dalı	Elektrik Elektronik Mühendisliği İngilizce	
Tez Konusu	Passive Islanding Detection Technique for Three-Phase Grid-Connected PV Inverter System	

Tez jüri üyeleri
Prof. Dr. Murtaza FARSADİ
Dr. Öğr. Üyesi Eylem Gülce ÇOKER
Prof. Dr. Ayşen DEMİRÖREN
Dr. Öğr. Üyesi Necip Gökhan KASAPOĞLU
Prof. Dr. Aydoğan OZDEMİR

Tezde kullanılan yöntem (birkaçının birden işaretleyebilirsiniz)

☐ Kuramsal ☒ Sayısal ☐ Deneysel ☐ Diğer:.....

Tez içeriği, Proje konusu ile uyuşuyor mu ? ☒ Evet ☐ Hayır

	Çok iyi	**İyi**	**Orta**	**Kötü**	**Çok kötü**
1.Tezde kullanılan yöntem uygun mu?	☐	☒	☐	☐	☐
2.Tez özgün mü?	☐	☒	☐	☐	☐
3.Tezdeki literatür taraması yeterli mi?	☒	☐	☐	☐	☐
4.Tezde kullanılan yöntemin güncelliği nasıl?	☒	☐	☐	☐	☐
5.Şekiller ve tablolar tezdeki bulguları yansıtıyor mu ?	☐	☒	☐	☐	☐
6.Tezde sunulan bulgular yeterince tartışılmış mı?	☒	☐	☐	☐	☐
7.Tezdeki bulgular, sonuçlar bölümünde iyi özetlenmiş mi?	☒	☐	☐	☐	☐

Tez hakkında verdiğiniz kararın gerekçelerini yazınız. (Gerekirse ek sayfa kullanınız.)

Tez kabulu konusundaki görüşünüz

☒ Değişikliğe gerek yoktur ☐ Şekil yönünden bazı değişiklikleri yapılması gerekir
☐ Reddedilmesi gerekir ☐ İçerik yönünden değişikliklere gerek vardır/yoktur

Öğretim Üyesinin

Adı Soyadı,Ünvanı	**Prof. Dr. Ayşen DEMİRÖREN**	
E-Posta		Tarih : 08.09.2021
Faks		
Telefon		Ayşen Demirören

92

T.C.
İSTANBUL AYDIN ÜNİVERSİTESİ
LİSANSÜSTÜ EĞİTİM ENSTİTÜ MÜDÜRLÜĞÜ

YÜKSEK LİSANS TEZ DEĞERLENDİRME FORMU

Adayın		**Tez Danışmanı**
Adı Soyadı	MOHAMMED YASSINE EL HASSNI	Prof. Dr. Murtaza FARSADİ
Numarası	Y1813.300011	
Anabilim Dalı	Elektrik Elektronik Mühendisliği	
Bilim Dalı	Elektrik Elektronik Mühendisliği İngilizce	
Tez Konusu	Passive Islanding Detection Technique for Three-Phase Grid-Connected PV Inverter System	

Tez jüri üyeleri
Prof. Dr. Murtaza FARSADİ
Dr. Öğr. Üyesi Eylem Gülce ÇOKER
Prof. Dr. Ayşen DEMİRÖREN
Dr. Öğr. Üyesi Necip Gökhan KASAPOĞLU
Prof. Dr. Aydoğan ÖZDEMİR

Tezde kullanılan yöntem (birkaçının birden işaretleyebilirsiniz)

☐ Kuramsal ■ Sayısal ☐ Deneysel ☐ Diğer:.....

Tez içeriği, Proje konusu ile uyuşuyor mu ? ■ Evet ☐ Hayır

	Çok iyi	**İyi**	**Orta**	**Kötü**	**Çok kötü**
1.Tezde kullanılan yöntem uygun mu?	■	☐	☐	☐	☐
2.Tez özgün mü?	☐	■	☐	☐	☐
3.Tezdeki literatür taraması yeterli mi?	☐	■	☐	☐	☐
4.Tezde kullanılan yöntemin güncelliği nasıl?	■	☐	☐	☐	☐
5.Şekiller ve tablolar tezdeki bulguları yansıtıyor mu ?	■	☐	☐	☐	☐
6.Tezde sunulan bulgular yeterince tartışılmış mı?	☐	■	☐	☐	☐
7.Tezdeki bulgular, sonuçlar bölümünde iyi özetlenmiş mi?	☐	■	☐	☐	☐

Tez hakkında verdiğiniz kararın gerekçelerini yazınız. (Gerekirse ek sayfa kullanınız.)

Başarılı.

Tez kabulu konusundaki görüşünüz

■ Değişikliğe gerek yoktur ☐ Şekil yönünden bazı değişiklikleri yapılması gerekir
☐ Reddedilmesi gerekir ☐ İçerik yönünden değişikliklere gerek vardır/yoktur

Öğretim Üyesinin

Adı Soyadı,Ünvanı	**Dr. Öğr. Üyesi Eylem Gülce ÇOKER**	
E-Posta		Tarih : 08.09.2021
Faks	:	
Telefon	:	İmza :

RESUME

Name Surname: Mohammed-Yassine El Hassni